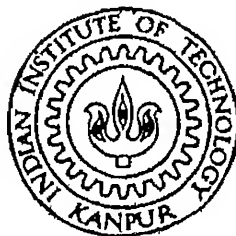


COMPARISON OF EXPERIMENTAL CYCLIC RESPONSE OF RC FRAMES WITH AND WITHOUT BRICK MASONRY INFILLS

by

Neeraj Kumar Vasandani

CE
1997
M
VAS
COM



DEPARTMENT OF CIVIL ENGINEERING

INDIAN INSTITUTE OF TECHNOLOGY KANPUR

December, 1997

**COMPARISON OF EXPERIMENTAL CYCLIC
RESPONSE OF RC FRAMES WITH AND WITHOUT
BRICK MASONRY INFILLS**

*A Thesis Submitted
In Partial Fulfilment of the Requirements
for the Degree of*
MASTER OF TECHNOLOGY

by
Neeraj Kumar Vasandani

to the
Department of Civil Engineering
INDIAN INSTITUTE OF TECHNOLOGY KANPUR
December, 1997

5 MAR 1998 /CI
CENTRAL LIBRARY
II KANPUR

Inv. No. A125010.

CE-1997-M-VAS-COM

Entered in System

On
64 98



A125010

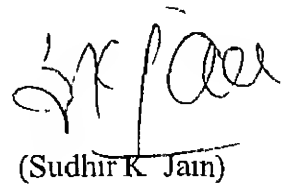
CERTIFICATE

It is certified that the work contained in the thesis entitled "**Comparison of Experimental Cyclic Response of RC Frames with and without Brick Masonry Infills**" by Neeraj Kumar Vasandani, has been carried out under our supervision and that this work has not been submitted elsewhere for a degree

November, 1997


(C. V. R. Murty)

Assistant Professor


(Sudhir K. Jain)

Professor

ABSTRACT

In the past four decades, significant research effort has been expended in studying the behaviour of masonry infilled RC frames. And, it has been recognised that the infills enhance the in-plane lateral stiffness and strength of the reinforced concrete frames. In literature, most of the experimental work on infilled frames is focussed on monotonic loading. And, in most of the work reported on behaviour of infilled frames under cyclic loading, attention is drawn primarily to the effect of various strengthening techniques and types of infills on lateral strength and lateral stiffness of the frame. In particular, very little work has been reported on the behaviour of infilled frames in India under reversed cyclic loading. So, in this study, cyclic testing of infilled frames is carried out to help the process of development of design guidelines for RC frames in India, which requires extensive experimental data.

In the present investigation, two single-storey one-bay reinforced concrete frames, one with complete brick masonry infill and the other without any infill, are tested under pseudo-static reversed cyclic lateral loading. The cyclic lateral load is applied at the beam level; no vertical or out-of-plane loads are applied on the frame. The strength and stiffness of the infilled and the bare frame are estimated using analytical models available in literature, and compared with experimental quantities. Also, stiffness degradation, strength deterioration, strain in reinforcement bars, overall frame ductility and energy dissipation in the two frames are compared. The experimental results indicate a beneficial influence of infills on the lateral load resistance of RC frames.

ACKNOWLEDGEMENTS

I wish to express my sincere thanks and gratitude to my advisors, **Prof. Sudhir K. Jain** and **Dr. C. V. R. Murty**, for their valuable guidance, continuous encouragement and kind hearted affection throughout my thesis course. I am deeply indebted to them for their timely help and suggestions on both academic and non-academic matters.

I am deeply indebted to **Dr. Durgesh Roy** for finding out his crucial time for me. I also express my gratitude towards all the faculty members of IITK who taught me during the course work. I am deeply grateful to **Mr. K. K. Bajpai** for his unforgettable love, affection and help provided for me.

I am deeply indebted to the staff members of the structural engineering lab, **Mr. Satyanatayana**, **Mr. Uday Singh**, **Mr. Devendra**, **Mr. Girvar** and **Mr. Satpal** for extending their full support in executing the experimental work. My special thanks are towards **Mr. Verma** and **Mr. Jaimangal** of machine shop.

I am deeply indebted to all my family members for the love, affection, and moral support I received from them. I am grateful to **Jaswant**, **Sreekanth**, **Rakesh** and **Sandy** for having brotherly affection toward me.

I pay my sincere thanks to **Moti**, **Pappu** and all of my friends. I will always cherish the moments spent with them.

Finally I thank **Lord Shiva** for every moment of my life.

TABLE OF CONTENTS

	<i>Page</i>
<i>Abstract</i>	ii
<i>Acknowledgements</i>	iii
<i>Table of Contents</i>	iv
<i>List of Tables</i>	vi
<i>List of Figures</i>	vii
<i>List of Symbols</i>	ix
1. INTRODUCTION	
1 1 General	1
1 2 Literature Review	3
1 2 1 Analytical Research	3
1 2 2 Experimental Investigations	7
1 3 Scope of Present Study	12
1.4 Organisation of the Thesis	12
2. EXPERIMENTAL STUDY	
2 1 General	13
2 2 Design and Fabrication of Test Specimen	13
2 3 Test Setup	14
2.4 On-line Data Acquisition	15
2 5 Loading	16
2 6 Test on Materials	17
3. RESULTS AND DISSCUSION	
3 1 General	19
3.2 Theoretical Estimates of Strength and Stiffness	19
3 2 1 Frame With Masonry Infill Wall (MRF 1)	21
3 2 2 Frame Without Infill (MRF 2)	29
3 3 Experimental Observations on Frames	29
3 3 1 Frame With Infill (MRF 1)	29
3 3 2 Frame Without Infill (MRF 2)	31

3 4 Discussion of Experimental Results	31
3 4 1 Load Displacement Response	31
3 4 2 Strength	32
3 4 3 Stiffness	33
3 4 4 Ductility	34
3 4 5 Energy Dissipation Capacity	35
3 4 6 Strain	35
3.5 Concluding Remarks	37
4. SUMMARY AND CONCLUSIONS	
4 1 Summary	40
4 2 Conclusions	40
4 3 Scope of Further Work	41
 <i>References</i>	 43
<i>Tables</i>	46
<i>Figures</i>	50
<i>Appendix-A</i>	69

LIST OF TABLES

<i>Table</i>	<i>Title</i>	<i>Page</i>
2 1	Quantities of materials used in MRF 1 and MRF 2	46
2 2	Properties of cement used in MRF 1 and MRF 2	46
2 3	Properties of bricks used in the construction of the infill panel	46
2 4	Average cube compressive strength of cement mortar used in MRF 1	46
2 5	Average cube compressive strengths of concretes used in MRF 1 and MRF 2	46
2 6	Tensile tests on steel reinforcement bars used in MRF1 and MRF 2	47
3 1	Analytical estimates and experimental values of stiffness and strength of MRF 1 and MRF 2	47
3 2	Strength deterioration in MRF 1 and MRF 2 as a percentage of strength in initial cycle.	48
3 3	Stiffness degradation in MRF 1 and MRF 2 as a percentage of average cycle stiffness in first cycle	49
3 4	Ductility factor of MRF 1 and MRF 2 at different displacement excusion levels	49
A	Variation of applied displacements with net displacements for MRF 1 and MRF 2.	70

LIST OF FIGURES

<i>Figure</i>	<i>Title</i>	<i>Page</i>
1 1	A typical planar RC moment resisting frame with unreinforced brick masonry infills	50
1 2	Separation between infill and RC frame member and strut action in infill (Drysdale <i>et al</i> ,1993)	50
1 3	Effective width-vs-relative stiffness curves for frames of different aspect ratios (Smith, 1967)	51
1 4	Diagonal strut action with notations (Drysdale <i>et al</i> , 1993)	51
2 1	Geometry of the two frames tested.	52
2 2	Details of reinforcement bars in MRF 1 and MRF 2	53
2 3	External dimensions of the wooden mould for casting the RC frame specimen	54
2 4	A view of the general arrangements of the specimen, the loading frame and the supports	54
2 5	A closer view of collar around the frame at the beam level to apply reversed cyclic displacement history	55
2 6	A schematic of the frame showing locations of LVDTs at which displacements are measured	55
2 7	A schematic of the frame showing locations of strain gauges pasted on the longitudinal reinforcement bars in MRF 1	56
2.8	A schematic of the frame showing locations of strain gauges pasted on the longitudinal reinforcement bars in MRF 2	57
2 9	Cyclic displacement history applied on (a) MRF 1, and (b) MRF 2.	58
3 1	Modulus of elasticity of masonry obtained from experiments reported in literature (Drysdale <i>et al</i> , 1993)	59
3 2	Idealized stress-strain curves for concrete and Fe415 steel	60
3.3	Finite element modelling for infill frame for different support conditions using SAP2000.	60
3 4	Finite element modelling for bare frame for different support conditions using SAP2000.	60
3.5	Final failure pattern for MRF 1	61
3 6	Final failure pattern for MRF 2	61

3 7	Lateral load versus lateral displacement hysteresis curves for (a) MRF 1, and (b) MRF 2	62
3 8	Schematic representation of (a) Initial stiffness, (b) Average cycle stiffness and (c) Ductility factor for a cycle	63
3 9	Envelope backbone curve of the load displacement hysteresis envelopes of (a) MRF 1 and (b) MRF 2	61
3 10	Effect of displacement excursion level on energy dissipated in MRF 1 and MRF 2 shown as (a) Cumulative energy dissipated upto that level of displacement excursion, and (b) Cumulative energy dissipated normalised with monotonic elastic energy upto yield	63
3 11	Lateral Load versus bar strain hysteresis curves for reinforcing bars in MRF 1.	64
3 12	Lateral Load versus bar strain hysteresis curves for reinforcing bars in MRF 2	65
A	Plot of LVDT3 data with load for (a) MRF 1, and (b) MRF 2	71

LIST OF SYMBOLS

<i>Symbols</i>	<i>Description</i>
A	Lateral flexibility related to axial deformation of the tension column
A_c	Area of cross-section of the column section
A_{sc}	Area of compression steel
A_{st}	Area of tension steel
A_{st}	Area of one stirrup (in column)
A_w	Horizontal cross sectional area of infill
b	Breadth of the column section
B	Lateral flexibility due to the diagonal strut
C	Lateral flexibility due to flexural deformation of the frame
d	Diagonal length of the infill panel
d'	Effective cover to the compression reinforcement
d_e	Effective depth of the column section
E_f	Modulus of elasticity of the reinforced concrete frame
E_m	Modulus of elasticity of the brick masonry
E_s	Modulus of elasticity of Fe415 steel
f_b	Compressive strength of Bricks
f_{ck}	Characteristic cube strength of concrete
f_m	Brick masonry strength
f_{ms}	14 day mortar strength
f_{sc}	Stress in compression reinforcement
f_{csc}	Stress in concrete at the level of centroid of compression steel
f_y	Yield strength of the main reinforcement
f_{yv}	Yield strength of the shear reinforcement
F_b	Flexural strength of the bare frame
F_c	Failure force for compression failure of diagonal strut
F_s	Failure force for the sliding shear failure of masonry
F_t	Failure force in tension failure mode

G_w	Shear modulus of the infill
h	Height of the reinforced concrete frame
h_w	Height of the infill wall
I	Moment of inertia of composite beam
I_b	Moment of inertia of beam of the reinforced concrete frame
I_c	Moment of inertia of column of the reinforced concrete frame
k	A factor adopted for evaluating modulus of elasticity of brick masonry for north American bricks
K_b	Lateral stiffness of the infill frame on basis of shear beam model
K_f	Lateral stiffness of the bare frame
K_{fl}	Flexural stiffness of composite beam
K_s	Lateral stiffness of the infill frame on basis of diagonal strut model
K_{sh}	Shear stiffness of composite beam
l	Length of the reinforced concrete frame
L_w	Length of the infill wall
m	Modular ratio, defined as E_f / E_b
M_u	Plastic moment capacity of the column section
R	Force in the compression diagonal strut
s_v	Spacing of shear reinforcement in columns
t	Thickness of the infill wall
V_u	Shear strength of column
w	Effective width of the diagonal strut
x_u	Location of the neutral axis in column section of the frame
Y	Diameter of Fe415 grade steel reinforcement bar (mm)
α	Length of contact between the wall and the frame
α_h	Length of contact between the wall and the column
α_l	Length of contact between the wall and the beam
β	Average stress factor of the non-linear concrete stress block
τ_c	Shear strength of concrete
γ_u	Location of centroid of concrete stress block

δ	Storey drift
Δ	Maximum displacement in a cycle
Δ_y	Yield displacement of the frame
ϕ	Diameter of the mild steel reinforcement bar (mm)
θ	Angle between the diagonal strut and horizontal axis
λh	Non-dimensional parameter, representing the relative stiffness of infill with respect to that of the frame
μ	Coefficient of friction for brick masonry
ν	Poisson's ratio for brick masonry
ε_c	Concrete compression strain in the extreme fiber
ε_{csc}	Compressive strain in concrete at the level of steel on the compression side
ε_s	Tensile strain in steel on tension side

Chapter 1

INTRODUCTION

1.1 General

Multistorey buildings with reinforced concrete (RC) moment resisting frames (MRF) infilled with unreinforced brick masonry walls are very common in India and in other developing countries (Figure 1.1). The loads are primarily resisted by the frame members (beams, columns, slabs). When the frame tries to deform under these loads, the masonry infill walls interfere with the frame. Thus, there is an interaction between the frame and the infill, which varies according to nature of interface between them. The interface surface depends on variety of factors like material, workmanship, and method of construction (Liau and Lee, 1977). Despite this obvious interaction, buildings are usually designed as bare frames with infills treated as non-structural components and the lateral load is assumed to be completely resisted by the frame alone.

In the last two decades, the contribution of the infill wall to the lateral stiffness and lateral load capacity of the frames has been recognized and considerable research work has been reported on the behaviour of infilled frames. Many reasons are attributed to the invalidity of “bare frame design approach” for design of frames with infills. Ambient vibration measurements of full scale prototype buildings have shown that the actual stiffness of reinforced concrete frame with infill is much higher than that of the corresponding “bare frame” (e.g., Jain *et al*, 1997). Experiences from the 1985 Mexico City earthquake show that, in many cases, infill walls have prevented collapse of buildings (Zarnic and Tomazevic, 1988).

In general, all frame panels in a building do not have infills, in fact, infills are located according to functional needs. The random location of infills and the varying sizes of openings in them give rise to sudden changes in stiffness along the frame, this results in an uneven distribution of the seismic shear resistance. This non-uniformity may develop significant torsional moment on the building, causing increased shear force in certain elements of the building.

Under strong ground shaking during earthquake, the brittle failure of the unreinforced infills causes a sudden transfer of shear force to the frame columns. Thus, the strength and ductility demand in columns becomes important. However, it is reported that the overall ductility demand on frame columns may be reduced because of the presence of infills (Nagar, 1995). Owing to the larger initial stiffness, the infilled frames will attract higher earthquake loads than the bare frames. Therefore, these increased loads should be accounted for in the design of the structure. The increased strength of infilled frames will significantly influence the inelastic behaviour of the structure. This needs to be considered while specifying the response reduction factors in seismic design. Thus, the increased stiffness and lateral load capacity on account of the infills seem to be beneficial in the seismic design of RC frames. Hence, a need arises to evolve a design approach for the seismic design of RC frames with brick infills which considers the strength and stiffness contributions of infills.

The Indian seismic code (IS 1893-1984) assigns a performance factor of 1.6 in the design of moment resistant frames with brick masonry infill, provided the infill panels are taken into consideration in stiffness as well as strength calculations and provided that the frame acting alone can resist, at least, twenty-five percent of the design base shear. In effect, the contribution of brick infills is implicitly included in the seismic design of buildings. An explicit approach is yet to be adopted in the Indian seismic code to consider

the contribution of infills. The development of such a design approach requires extensive data from experimental investigations. The present study is a step in this direction.

1.2 Literature Review

1.2.1 Analytical Research

Efforts towards more realistic analysis of infilled frames have been reported since the 1950's. The initial studies were largely limited to the modeling of lateral stiffness of infill masonry. In this connection, some approximate methods were proposed for predicting lateral stiffness and strength of infilled frames on the basis of simple beam theory (Whitney *et al*, 1955). The infill masonry walls in RC MRFs have often been treated as equivalent diagonal members running between the beam-column joints. The stiffness of the infilled frame is modeled assuming the infill to behave as a diagonal strut. This diagonal strut analogy was motivated by the observation of separation between the frame and the infill at the two tension corners (Figure 1.2). The diagonal strut approach was then used to include the effect of variation in stiffnesses of frame and infill, and a non-dimensional parameter (λh), representing the relative stiffness of infill to frame was defined (Smith, 1962, Smith, 1966). The effect of multi-panel interaction was also taken into account in these studies.

A design method based on equivalent strut concept was developed (Smith and Carter, 1969) to account for the lateral stiffness of infilled frame under monotonic loading. In this design method, "beam on elastic foundation" approach was used to obtain length of contact between the frame and the infill. Design charts were provided to calculate the cracking and crushing strength of brick masonry panels. Further, it was observed that the combined action of frame and infill in resisting lateral load can be much greater than the sum of the individual resistances of frame and infill (Smolira, 1973). The effectiveness of

combined action depends on many complex parameters like quality of material, workmanship, and interspace between frame and infill. Mathematical expressions were developed for the frames with tightly fitting infill and for frames with interface spaces.

Researchers have given different formulae for estimating the geometrical properties of the equivalent diagonal strut for single-storey one-bay portal frames with infills. One relation (Smith, 1966) between the contact length α and a non-dimensional parameter λh representing relative stiffness of infill and frame is

$$\frac{\alpha}{h} = \frac{\pi}{2\lambda h} = \frac{\pi}{h} \left(\frac{E_f I_c h}{4E_m t \sin 2\theta} \right)^{1/4}, \quad (1.1)$$

where E_f and E_m are the moduli of elasticity of the frame members and the infill, respectively, I_c is the moment of inertia of the column section, h is the height of the frame, t is the thickness of the infill, and θ is the angle of the frame diagonal with respect to a horizontal axis. A set of empirical curves relating the relative stiffness parameter λh to the effective width w of the equivalent strut (Figure 1.3) were also provided therein. Other expressions for w given by different researchers are

$$w = \begin{cases} \frac{d}{3} & \text{from Holmes, 1963} & (1.2) \\ 0.175(2L_w \sin \theta)(\lambda h)^{-0.4} & \text{from Mainstone and Weeks, 1970} & (1.3) \\ \frac{\sqrt{\alpha_l^2 + \alpha_h^2}}{2} & \text{from Hendry, 1981} & (1.4) \\ 0.25d & \text{from Paulay and Priestley, 1992} & (1.5) \end{cases}$$

In Eqs (1.2) and (1.5), d is the diagonal length of the infill panel. In Eq (1.3), L_w is the length of infill wall. In Eq (1.4), α_l and α_h are the lengths of contact between the wall and the beam and between the wall and the column, respectively (Figure 1.4), and are given by

$$\alpha_l = \pi \left(\frac{4E_f I_b L_w}{E_m t \sin 2\theta} \right)^{1/4} \quad \text{and} \quad (1.6)$$

$$\alpha_h = \frac{\pi}{2} \left(\frac{4E_f I_c h_w}{E_m t \sin 2\theta} \right)^{1/4} \quad (1.7)$$

where h_w is the height of infill panel, and I_b is the moment of inertia of beam

In another study, a simple analytical procedure for the seismic design of masonry infilled frame was presented (Kodur *et al*, 1994). According to the study, when the frame and infill act together, the combined action of the composite system differs significantly from that of the frame or the wall considered individually. As compared to the bare frame, the infilled frame may demonstrate enhanced lateral load resistance, improved lateral stability and smaller deformations. This increased resistance of the infilled frame can be attributed to the development of high axial forces and bending moments in the frame, and to the confinement of the infill. The analysis procedure given in the study, accounts for the effect of infills in all the stages of the design process, namely, in computing seismic lateral load, in determining the forces in members, and in determining strength of the different components of the system. In case of infilled frame without openings, the frame was idealized by replacing infill with an equivalent diagonal strut pinned at its both the ends. The steps associated with the seismic design and analysis of infilled frame are presented below:

- (1) The preliminary design of frame is conducted and the seismic design response spectrum is established from design codes
- (2) The infilled frame is idealized and a free-vibration dynamic analysis is carried out to determine the dynamic characteristics of the structure, namely, natural periods and corresponding mode shapes.
- (3) The seismic design base shear is computed through modal analysis procedure
- (4) A static analysis of the infilled frame, with all loads, is performed and the member forces in the infill and the frame members are estimated.

- (5) The columns, beams, and infills are designed for these forces
- (6) The strengths of the members are estimated under different failure modes. If these strengths exceed design forces, the design is said to be safe. If the design forces exceed the strength, the member sizes are modified

Significant amount of studies were also performed by modelling the masonry wall panel as a planar continuum idealized as a collection of finite elements (Liauw and Lee, 1977, Ali and Page, 1987; King and Pandey, 1978). A method was proposed to ascertain the separation of frame from the infill wall, and the stress distribution along the contact intervals (Mallick and Severn, 1968). In the method, a stiffness matrix was developed by idealizing the infill as a plane-stress element and by considering frame members to be axially rigid

The interface between the frame and the infill was modeled on a finite element platform using friction elements (King and Pandey, 1978). It was shown that a fairly coarse finite element mesh can give results that are in good agreement with the experimental results. Another analytical model based on FEM was proposed for predicting the response of masonry infilled frames subjected to reversed cyclic loading (Michalidis *et al*, 1995). The model was based on the approach that the contribution of infill wall can be obtained by the subtracting the shear carried by a bare frame from shear carried by an identical frame with infills. Characteristics of hysteresis behaviour of the infill panel, strength deterioration, stiffness degradation, pinching and slippage were taken into account in the study. Seismic behaviour of frames with various arrangements of infill panel including an open ground storey, was used to investigate the influence of regular and irregular patterns of masonry infills. Frames with regular patterns of infills were generally found to demonstrate a superior behaviour compared to bare frames or frames

with irregular patterns of infills. Infill walls were found to provide the main energy dissipation mechanism in such structures subjected to cyclic loading

1.2.2 Experimental Investigations

A large amount of experimental work has been done to study the behaviour of infilled frames. Several experimental tests were conducted on four-storey infilled steel frames, with and without openings and with and without connectors between the frame and the infills (Liau and Lee, 1977; Liau, 1979). Reduced scale models of approximately 1:12 were constructed. The size of infill used was 305mm×610mm×22mm and the cross-section of steel frame was 22mm×22mm. These tests studied the use of micro-concrete wall as infill panel. A horizontal loading system was adopted with the model set up vertically and a concentrated load was applied horizontally at the top through a pulsator jack with a maximum capacity of 100 kN load. Comparisons of the experimental results were made with analytical estimates of stiffness and strength. Use of diagonal strut approach was found justified for predicting behaviour of infilled frames subjected to lateral loads, except when large openings are present. The contribution of infills to the lateral strength and stiffness of infilled frames was found to be very significant. The provision of shear connectors increased the strength and stiffness of infilled frame. Presence of openings in infills was found to considerably reduce the capacity of the structure to withstand dynamic loading.

Experimental studies on masonry infilled RC frames subjected to cyclic lateral loading have also been reported in literature. In one of these studies (Zamic and Tomazevic, 1984), four single-bay single-storey specimens were constructed to 1:2 reduced scale. These include three types of specimens, namely bare frame, frame with unreinforced infill, and frame with reinforced infill. The specimens were subjected to a

constant vertical load acting on each column and a cyclic horizontal load acting on the beam. The study concluded that infilled frames behave as a single structural system till the cracking of infills. After cracking, the frame takes over a significant part of the lateral load, until its columns fail in shear. A small amount of reinforcement (0.2%) in the infill was found not to influence the lateral resistance or ductility, increase in the lateral resistance was observed when infill reinforcement was anchored in the frame members.

In another study (Zarnic and Tomazevic, 1988), the effect of different types of unreinforced and reinforced infills on lateral strength, lateral stiffness, ductility, strength deterioration, stiffness degradation, energy absorption and dissipation capacity, were investigated. Lateral strength and stiffness of infilled frames were observed to be significantly greater than those of bare frames, and both of these properties were found to depend on quality of infill material, contact between frame and infill wall, and opening in the infill. The infill reinforcement significantly influenced the specimen behaviour in case of infill frame with openings. The infilled frames damaged by cyclic testing were repaired and strengthened by various methods. Epoxy grouting and RC coating of infill significantly improved the stiffness and load bearing capacity.

Some experimental parametric studies were also made on the behaviour of infilled frame. In one of these studies (Pires and Carvalho, 1992), six single-storey single-bay RC frames were constructed to 1:1.5 reduced scale, in which brick masonry walls were used as infills. The parameters investigated were (a) connection conditions between frame and infill, (b) anchorage of longitudinal reinforcement of beam and columns, (c) spacing of hooks and stirrups in zones contiguous to the joints, (d) longitudinal reinforcement ratio in columns, and (e) mechanical character of masonry infills. It was found that after the first cracking, the infill was divided into two zones. One zone was oriented along the diagonal of the infill, while the remaining portion of the infill formed the other. The initial

stiffness and maximum strength were found to depend on construction procedure and shear strength of infills. The difference in reinforcement did not influence these.

In another experimental parametric study, eleven single-storey single-bay frames were constructed at the reduced scale of 1/2 (Schuller *et al*, 1994a). A six-storey, three-bay RC frame was selected as a prototype structure. The cyclic lateral load was applied by means of two servo-controlled hydraulic actuators, each of which had a load capacity of about 500 kN and a stroke of ± 125 mm. Concrete masonry blocks were used in the infill masonry. The effect of the influence of relative strength of infill panels and bounding frame, and influence of aspect ratio were investigated. The strength of infilled frame was found to be 1.5 to 2.3 times that of the bare frame, while the stiffness was 15 to 50 times that of the bare frame. The aspect ratio (height-to-length ratio) was found to have little effect on ductility and strength of the frame, frame with smaller aspect ratio was found to be slightly stronger. An extension of the study with a few more interesting parameters like lateral displacement histories, distribution of vertical load and influence of adjacent infilled bays was reported in another publication (Schuller *et al*, 1994b). It was observed that monotonically loaded specimens have higher load resistance about 1.1 to 1.7 times as compared to those which are cyclically loaded.

Tests were performed on fourteen two-storey one-bay RC frames with concrete walls as infills under reversed cyclic loading (Altın *et al*, 1992). The objective of the study was to investigate the behaviour of infill frames under seismic loads. Cyclic lateral load was applied only at the top of the second storey. The test variables included configuration of infill reinforcement, connection between frame and infill, and flexural capacity of columns. The ultimate strength and the behaviour of infilled frame were not found to be affected by the pattern of the reinforcement used in infill, provided the

amount of reinforcement was kept same. Introduction of infill panels into the frame of a building significantly altered the dynamic characteristics of the building.

Experiments were conducted on four three-storey one-bay infilled frames and one three-storey one-bay bare frame subjected to reversed cyclic loading (Gaunlovic and Sendova, 1992). Four types of infill materials (brick masonry, syporex, eltozol and gypsum) were used for the infilled frames. These structures were constructed to 1:2 reduced scale. The strength and stiffness of infilled frames were found higher than those of the corresponding bare frame. After cracking, significant strength deterioration and stiffness degradation were observed. A series of pseudo-dynamic tests were conducted on full-scale four-storey RC buildings (Vegro and Verzeletti, 1996). Tests were conducted on the bare frame as well as on the frame with the different configurations of non-structural masonry infills. It was seen that presence of light non-structural infills can change response of structure to a large extent and that regular pattern of infills prevents energy dissipation from taking place in the frame. It was also observed that irregular infill patterns in the structure resulted in unacceptably large damage in frames.

A number of studies have shown that the properties of the infill material significantly influence the overall behaviour of infilled frame. Investigations on strength and related properties of brick masonry are also reported in literature. In one study (Grimm, 1975), relationships between sixteen controllable variables (which affect compressive, flexural, and shear strength of brick masonry) were presented in the form of ten empirical equations. The factors influencing brick compressive strength, mortar compressive strength, brick masonry compressive strength and flexural strength were also discussed. In another study (Dhansekar and Page, 1986), the influence of brick masonry infill properties on the behaviour of infilled frame was investigated. It concluded that behavior of infill frame not only depends on relative stiffness of frame and infill, and on

frame geometry, but also on the strength-related properties of masonry. Modulus of elasticity of masonry was also reported to significantly influence the load-deflection behavior of frame and to a lesser extent its ultimate strength.

From the above review of literature, it is clear that many theoretical and experimental investigations have been carried out on the behaviour of infilled frames. However, inspite of these efforts, specific guidelines are not yet available for the design of infilled frames and a complete solution to the problem of defining the degree of contribution of infill to the lateral stability of building has not yet been evolved. In the available literature, most of the work is focused on monotonic load conditions and in most of the work reported on behaviour of infilled frames under cyclic/reversed cyclic loading, attention is given primarily to investigate the effect of various strengthening techniques and addition of different types of infills on lateral stiffness of frame. Very little work has been reported on the behaviour of infilled frames under reversed cycles of loading. Theoretical analysis attempted by some investigators on the basis of their experimental results could not draw much appreciation owing to the variations in quality of bricks and mortar, in workmanship, shrinkage or moisture expansion of brickwork, *etc.*, (Achintya *et al*, 1991). Even though a number of studies have been conducted on infilled frames, experimental data which can be used for assessing the performance of such structures are still very limited (Choubey, 1990; Schuller *et al*, 1994b). Most of the early tests were conducted on the small-scale structures. So the need of the hour is to carry out cyclic load tests on infilled frames for getting reliable test data in order to enrich the literature on experimental work; this will aid the development of design guidelines or expressions, which requires extensive data from experimental investigations. The present study is a step in that direction. The objective of the present investigation is to compare the performances of single-bay single-storey reinforced concrete infilled and bare frames

under cyclic load conditions from the point of view of lateral load carrying capacity, load-deflection behaviour, load-strain behaviour, stiffness degradation, strength deterioration, ductility and energy dissipation

1.3 Scope of Present Study

The basic objective of present investigation is to study the hysteretic behavior of reinforced concrete frames with and without brick masonry infill under pseudo-static reversed cyclic loading of displacement-control type. The frames studied are of one-bay single-storey type. The cyclic lateral load is applied horizontally at the beam level at the top of the frame. No vertical loads or out of plane loads are applied on the frame. The frames tested include a frame with complete infill, and an identical but bare frame.

The properties of materials used in frame and infill wall are experimentally obtained. Analytical estimates of the strength and stiffness of infilled frames are obtained based on models available in the literature. Estimates of elastic stiffness are obtained using a standard FEM package. These analytical quantities are compared with the experimental results to draw conclusions.

1.4 Organization of the Thesis

The contention of this thesis is presented in five relatively independent chapters. Chapter 1 introduces subject matter of this study and reviews the associated literature. The various stages of the experimental program such as design and fabrication of test specimen, experimental set-up and testing are described in Chapter 2. The experimental results and analytical estimates are presented in Chapter 3. Finally, the main conclusions of this study are stated in Chapter 4.

Chapter 2

EXPERIMENTAL STUDY

2.1 General

The experimental work reported in this study is presented in four segments. The first segment involves design and fabrication of the test specimen. In the second segment, properties of the materials used in the fabrication of the specimen are ascertained through standard material tests. The third segment consists of preparation of experimental setup for cyclic testing of specimens. In the fourth segment, the experimental investigation of the cyclic behaviour of the RC frames is conducted.

2.2 Design and Fabrication of Test Specimen

The two single-bay single-storey RC frames studied are shown in Figure 2.1. The first one is a RC frame with infill (MRF 1) and the other is a bare RC frame (MRF 2). A 1/27 geometrically-reduced scale model of typical prototype frames is adopted. The cross-sections of members are same in both frames, the columns are 115mm×200mm and beam is 115mm×200mm. To create a complete rotational restraint at the base of the columns, a base beam of size 200mm×400mm is cast monolithically with the portal frame. The reinforcement details in the frame are shown in Figure 2.2. Again, these are same in both the frames. For measuring strain in the reinforcement bars, 120Ω linear resistance strain gauges (Model SR-4, manufactured by m/s BLH Electronics, USA, gauge length 7 mm, gauge factor 1.96) are used.

The specimens are cast in the horizontal position and tilted up to the vertical position. A wooden mould made of 20 mm plyboard (Figure 2.3) is used to cast the specimens. The side forms of mould are held in position with wooden spacers to prevent bulging during placing and vibration of concrete. Before concreting, plaster of Paris is used to fill gaps at all joints to prevent leakage of the cement paste during vibration of concrete. Further, the mould is well oiled with mould oil.

The reinforcement cage is prepared as per the details given in Figure 2.2. A concrete mix of 1 : 1.84 : 3.55 (cement : sand : aggregate) by weight with a water-cement ratio of 0.52 is used. The same mix proportions are used in both the specimens. Owing to limitations in the size of the available tilting-type revolving-drum concrete mixer, the concrete is mixed in four batches of 0.15 m³ each. The quantities of materials used in the casting are shown in Table 2.1. The concrete is placed in the mould along with six standard 150 mm cube moulds. A needle vibrator is carefully employed to vibrate the concrete.

The side forms of the mould are detached after 24 hours. The specimen is covered with gunny bags, these are kept wet by regular watering. After 7 days, the specimen is moved laterally to free the base of the mould, the mould was re-assembled for casting the next frame. Each specimen and its standard cubes are cured under the same conditions for 28 days. The frame specimen is tilted up to the vertical position after 28 days and moved to the structural floor for testing.

2.3 Test Setup

The frame specimen is secured to the structural floor with clamps on the base beam using 40 mm diameter studs (Figure 2.4). In case of MRF 1, a half-brick wall (115 mm

thick) is raised within the 1800mm×1000mm opening between the columns and beam. This unreinforced brick masonry panel is constructed with 224 mm×110 mm×67 mm size bricks bonded together with a cement mortar of 1:6 proportion by weight. The wall thickness matches with the width of the top beam and columns. The brick masonry infill of MRF 1 is cured for 14 days by regularly sprinkling water on the surface. A 250 kN capacity MTS hydraulic dynamic actuator is used to apply the cyclic displacement history on the frame specimen. The push and pull action under cyclic conditions is achieved through the collar arrangements around the frame as shown in Figure 2.5. The push displacement is taken as positive and the pull displacement as negative.

2.4 On-line Data Acquisition

The deflections in the specimen are measured with Linearly Variable Displacement Transducers (LVDTs), which produce voltage signals proportional to the displacement at the point of measurement. Five LVDTs are used at the locations shown in Figure 2.6. LVDT 1 is used to measure displacement at beam level and LVDT 2 is used to measure displacement at mid-height of the column. The lateral displacement of the back support to the hydraulic actuator is measured using LVDT 3. The slip of the specimen at its base is measured through LVDT 4. The vertical uplift, if any, at the base beam is obtained from LVDT 5. The LVDTs 1 and 2 are of ± 50 mm range, and LVDTs 3, 4 and 5 are of ± 25 mm range. Twenty-four strain gauges are pasted to the bars in each of the two frames at locations shown in Figures 2.7 and 2.8. After concreting operations, six strain gauges in MRF 1 and eight strain gauges in MRF 2 were found out of order. However, only ten of them could be monitored during experiments because of the following reasons:

- (i) The lead wires of some of the strain gauges were broken during handling.

- (ii) The wheatstone bridge circuit was fabricated on a small PCB, without provision of proper bridge balancing facility, which causes saturation of some of the ADC board channels

The readings of strain gauges 1, 2, 3, 9, 14, 15, 17, 19, 20 and 21 in MRF 1, and strain gauges 4, 10, 12, 14, 15, 17, 18, 19, 23, and 24 in MRF 2 were recorded. The LVDT and strain gauge readings at each loading point are directly recorded on a personal computer PC 386 through an on-line 12 bit data acquisition system. A quarter bridge configuration is used for the strain gauges in the data acquisition system. Available software, that was developed in-house at IIT Kanpur, for PCL-208 data acquisition card with PCLD-770 signal conditioning board and PCLD-7702 plug-in signal conditioning module carrier board, is used in this study.

2.5 Loading

A cyclic lateral load is applied on the specimen through the hydraulic actuator under displacement control. Displacement controlled loading is employed to track the post-yield behaviour. The expected yield displacement is obtained as 0.36 mm for MRF 1 and 2.4 mm for MRF 2 using the analytical values of failure load and elastic stiffness computed by SAP2000. The applied displacement history is shown in Figure 2.9. The loading cycles adopted for MRF 1 are of ± 1 mm, ± 2 mm, ± 3 mm, ± 5 mm, ± 7.5 mm, ± 10 mm, ± 15 mm, ± 25 mm and ± 40 mm amplitudes, and those for MRF 2 are of ± 1 mm, ± 2 mm, ± 3 mm, ± 4 mm, ± 5 mm, ± 7.5 mm, ± 10 mm, ± 15 mm and ± 25 mm amplitudes. The same displacement level was repeated three times to study strength deterioration and stiffness degradation in the frames under repeated loading.

2.6 Test on Materials

The materials used in the RC frame and the brick masonry infill are tested as per Indian Standard specifications to obtain their properties. The properties of cement are ascertained through tests specified in IS 4031-1976, the results are shown in Table 2.2. The same cement is used for the both RC frames concrete and masonry mortar.

First class well-burnt bricks are used in brick masonry work in MRF-1. The dimensional characteristics of brick are studied as per IS 1077-1976, and the average dimensions of bricks are given in Table 2.3. The compressive strength tests on bricks are performed as per IS 3495 (Part 1)-1976. Five samples of brick are soaked in water for a day before filling the frog with 1:2 cement sand grout. The bricks are again soaked in water for three days before testing. The compressive strength of the bricks is also shown in Table 2.3. The water absorption test of bricks is performed as specified by IS 3495 (Part 2)-1976. Five oven-dried bricks are weighed, immersed in water for 24 hours, and weighed again. The difference in weight is a measure of the amount of water absorbed (Table 2.3). The average water absorption is found to be 15.3% by weight, which is within the permissible limit (20%) as specified by IS 1077-1976 for well burnt first-class bricks.

A cement mortar of 1:6 (cement : sand) proportion by weight is used in the brick masonry work. Standard cubes of 75 mm size of this mortar are tested for their 3-day, 7-day and 14-day compression strengths. These strengths are given in Table 2.4. The average 3-day, 7-day, and 14-day mortar strength is 4.7 MPa, 7.7 MPa, and 11.4 MPa, respectively.

Along with each RC frame, six standard cubes of 150 mm size are cast to determine the compressive strength of the concrete. Three cubes are tested after 28 days and three more on the day of testing of the frame. The results are given in Table 2.5. The

average 28-days cube strengths are found as 31.5 MPa for MRF 1, and 29.9 MPa for MRF 2.

The longitudinal reinforcement used in frame is of high yield strength deformed (HYSD) bar type (Fe415 grade) of 10 mm and 12 mm diameters. The stirrups are of 6 mm diameter mild steel (Fe250 grade). Uniaxial tension tests are conducted on two bars of each size as per IS 1786-1976. The test results are presented in Table 2.6. The 10 mm and 12 mm diameter HYSD bars are found to have 0.2% proof stress as 417 MPa, and 478 MPa, respectively.

• • •

Chapter 3

RESULTS AND DISCUSSION

3.1 General

The results of cyclic lateral load tests on RC frames with and without brick masonry infill are reported and discussed in this chapter. The ultimate strength of the infilled frame for different possible failure modes as per analytical methods available in literature are computed. The initial stiffness of the infilled frame is computed analytically by using equivalent diagonal strut model, shear beam model, and by using FEM package SAP2000 (Habibullah, 1995). Similarly, the strength and stiffness of bare frame are also computed. The experimentally obtained initial stiffness is compared with theoretical estimates. The “average cycle stiffness” is used as a measure to understand the extent of stiffness degradation. A comparison of stiffness, strength, deflection at peak strength, ductility and energy dissipation of MRF 1 and MRF 2 is presented.

3.2 Theoretical Estimates of Strength and Stiffness

The modulus of elasticity E_f (in MPa) of concrete is calculated using the relation (IS 456-1978)

$$E_f = 5700 \sqrt{f_{ck}}, \quad (3.1)$$

where f_{ck} is the 28-day cube strength of concrete. The average values of f_{ck} for MRF 1 and MRF 2 from Table 2.5 are obtained as 31.5 MPa and 29.9 MPa, respectively. Hence,

the modulus of elasticity of concrete is obtained as 32,000 MPa for MRF 1 and 31,100 MPa for MRF 2

The compressive strength f_m (in MPa) of brick masonry is calculated using the relation (Dayaratnam, 1987)

$$f_m = 0.289 \sqrt{f_b f_{ms}}, \quad (3.2)$$

where f_b and f_{ms} are the experimental compressive strengths of brick and 14-day masonry mortar, respectively. And, the modulus of elasticity E_m (in MPa) of brick masonry is calculated from the relation (Paulay and Priestley, 1992, Hart, 1989)

$$E_m = 750 f_m \quad (3.3)$$

From Tables 2.3 and 2.4, the experimentally obtained average values of f_b and f_{ms} are 18.7 MPa and 11.4 MPa, respectively. Hence, f_m and E_m are obtained as 4.2 MPa and 3,160 MPa, respectively.

It is difficult to specify accurately the modulus of elasticity of brick masonry. A number of relationships are available in the literature for modulus of elasticity of brick masonry, each relation giving a very different value. For instance, one study (Drysdalet al, 1993) recommends that

$$E_m = k f_m \quad (3.4)$$

where $k=500$ to 600 for masonry with north American bricks. This expression gives an E_m value of about 2,300 MPa, as compared to 3,160 MPa calculated using Eq.(3.3). The large scatter in modulus of elasticity for clay brick masonry and concrete masonry is evident from the experimental data shown in Figure 3.1

3.2.1 Frame With Brick Masonry Infill Wall (MRF 1)

(a) Strength

Different failure modes are possible for masonry infilled frames (e.g., Paulay and Priestley, 1992, Drysdale *et al.*, 1993). These include tension failure of column longitudinal reinforcement due to large axial tensile force, sliding shear failure of masonry, compression failure of diagonal strut, and flexural failure of columns due to development of large moments at column ends. In many cases, final failure may occur after a sequential combination of these modes. For example, flexural or shear failure of column generally follows a sliding shear failure or diagonal compression failure of masonry. For infilled frames, the strength associated with the various possible failure modes is evaluated individually, and the combination which gives the lowest lateral strength should be used as the basis of design. The maximum lateral load capacity for each of these failure modes is presented in Table 3.1.

(i) Tension Failure of Column

Under lateral loads on the frame, critical failure mode may involve tensile yield of steel in the tension column. This is generally observed in frames with large aspect ratio (i.e., height-to-length ratio). Here, the infilled frame acts as a cantilever wall, and a reasonably ductile failure mode can be expected. The lateral load capacity F_t is determined by dividing the tensile capacity of column by the aspect ratio. Hence,

$$F_t = \frac{A_{st} f_y}{(h/l)} \quad (3.5)$$

where A_{st} is the total area of longitudinal reinforcement in the column, f_y is the yield stress of reinforcement, h is the height of the frame and l is the length of the frame. For the frame at hand $A_{st} = 4 \times 78.5 \text{ mm}^2$, $f_y = 415 \text{ MPa}$, $h = 1,100 \text{ mm}$ and $l = 2,000 \text{ mm}$. Hence,

Eq (3.5) gives the lateral load capacity for tensile failure as 236.9 kN.

(ii) Sliding Shear Failure of Masonry (Cracking Load)

The lateral shear resistance of masonry is usually considered to be provided by the combined action of the bond between bricks and mortar, and shear strength of the mortar. In this mode, the infill wall fails in shear along the bed joint rather than by diagonal tension. The formation of shear cracks separates the panel into two parts so that effective column height reduces to approximately half. This type of failure occurs where the masonry has a low shear strength along the bed joints. The lateral load at which the first major sliding crack initiates in the infill, is also called the “*cracking load*”. At this instant, it is possible that plastic hinges may form at mid-height, top or bottom of the column. The maximum lateral load capacity for this type of failure can be obtained in the following manner. The maximum sliding shear force that can be resisted by the infill panel is (Paulay and Priestley, 1992)

$$F_s = 0.03 f_m L_w t + 0.3 R \sin \theta, \quad (3.6)$$

where shear stress in masonry is taken as $0.03 f_m$, coefficient of friction is taken as 0.3, R is the force in compression diagonal strut, L_w is the length of the infill wall, t is the thickness of the infill wall, and θ is the angle which the diagonal of infill wall makes with horizontal. The equilibrium between the horizontal component of the compression force R in the diagonal strut and the applied lateral force F_s demands that

$$F_s = R \cos \theta, \quad (3.7)$$

From Eqs (3.6) and (3.7), the maximum sliding shear force F_s is

$$F_s = \frac{0.03 f_m L_w t}{1 - 0.3(h/l)} \quad (3.8)$$

where h and l are the height and length of the frame, respectively. Again, for the infilled frame at hand, $f_m = 4.2$ MPa, $t = 115$ mm, $h = 1,100$ mm, $l = 2,000$ mm and $L_w = 1,800$ mm, and hence Eq (3.8) estimates the cracking load as 31.3 kN.

(iii) Compression Failure of Diagonal Strut

At low levels of in-plane lateral force, the frame and infill panel act in a fully composite fashion. As the lateral deformation increases, the behaviour becomes more complex, the frame attempts to deform through flexural action and the panel through shear action. This results in a separation between the frame and the panel at the corners along the tension diagonal, and in the development of a diagonal compression strut (Figure 1.3). Here, the ultimate lateral capacity F_c of the frame is governed by compressive strength of the strut and is given by the expression (Paulay and Priestley, 1992),

$$F_c = \frac{2}{3} \alpha_h f_m \sec \theta, \quad (3.9)$$

where α_h is defined as the vertical contact length between the panel and the column, and given by the expression (Paulay and Priestley, 1992, Drysdale *et al*, 1993)

$$\alpha_h = \frac{\pi}{2} \left(\frac{4E_f I_c h_w}{E_m t \sin 2\theta} \right)^{1/4} \quad (3.10)$$

I_c is the moment of inertia of concrete columns, h_w is the height of infill panel, and θ is the angle between the diagonal strut and the horizontal. For the frame at hand, $E_f = 32,000$ MPa, $I_c = 7.67 \times 10^7$ mm⁴, $h_w = 1,000$ mm, $f_m = 3,160$ MPa, $t = 115$ mm and $\theta = 29^\circ$. Thus, Eq (3.10) gives α_h as 663.3 mm. Using this value of α_h in Eq (3.9), F_c is obtained as 244.8 kN.

(iv) Flexural Failure of Frame

The flexural failure of the portal frame shown in Figure 2.1b occurs when plastic moment hinges develop at the top and bottom of the columns or at the bottom of the columns and at the beam ends. As plastic moment capacity M_u for the beam and column

sections are same, the maximum flexural strength I_b of frame is given by

$$I_b = \frac{4M_u}{h}, \quad (3.11)$$

where h is the height of the column M_u is obtained from basic principles of limit state design (IS 456-1978) as described below. The depth x_u of neutral axis for the column cross-section is computed by equating the compressive and tensile forces, as

$$\beta f_{ck} b x_u (f_{sc} - f_{csc}) A_{sc} = f_y A_{st}, \quad (3.12)$$

In Eq (3.12), it is assumed that the section is under-reinforced and hence the tension steel yields before concrete crushes on the compression side. The stress-strain curves of concrete and steel are taken as per IS 456-1978 (Figure 3.2). β is the average stress factor of the nonlinear concrete stress block. The strain relation is

$$\frac{\epsilon_c}{\epsilon_c + \left(0.002 + \frac{f_y}{E_s}\right)} = \frac{x_u}{d_e}, \quad (3.13)$$

From Eqs (3.12) and (3.13) and the stress-strain curves for concrete and steel, x_u is evaluated. Using the moment equilibrium at the section,

$$M_u = \beta f_{ck} b x_u \left(d_e - \gamma_{xu}\right) + (f_{sc} - f_{csc}) A_{sc} (d_e - d')$$
(3.14)

moment of resistance is calculated. Here γ_{xu} is the location of centroid of the concrete stress block and f_{csc} is the stress in concrete at the level of compression steel. An iterative procedure is followed so that for a particular value of x_u/d_e , the compressive force is equal to the tensile force. For the cross-section of the frames at hand, $x_u = 43.68$ mm, $\beta = 0.314$, $\epsilon_c = 0.00136$, $\epsilon_{csc} = 0.00058$, $f_{sc} = 116.4$ MPa, $A_{st} = A_{sc} = 2 \times 78.5$ mm², $f_{csc} = 11.95$ MPa, $d_e = 175$ mm, $d' = 25$ mm, $\gamma_{xu} = 15.44$ mm, $f_{ck} = 31.5$ MPa. Thus, from

Eq (3 14), the value of M_u is obtained as 10.4 kNm for infilled frame, and F_b as 37.8 kN

The shear capacity of each column is given by

$$V_u = \frac{\tau_c b d_e}{0.85} + \frac{f_{yv} A_{sv} d_e}{s_v} \quad (3 15)$$

For the frame at hand, concrete shear capacity $\tau_c = 0.6$ MPa, $b = 115$ mm, $d_e = 175$ mm, $f_{yv} = 250$ MPa, $A_{sv} = 56.52$ mm² and spacing $s_v = 75$ mm. On substituting these values in Eq (3 15), the shear capacity of the two columns is obtained as 94.4 kN, which is larger than the lateral strength of the bare frame obtained from flexural failure.

(v) Comparison

The final failure may be in tension failure mode, in form of compression failure of diagonal strut or in combination of sliding shear failure with flexural failure of columns (Table 3 1). The lowest value of failure force was obtained by taking combination of sliding shear failure (31.3 kN) followed by flexural failure of columns (37.8 kN). So lowest strength associated with failure is 69.1 kN.

(b) Stiffness

(i) Diagonal Strut Model

The infilled frame is idealized as a bare frame with the infill idealized as a diagonal member pinned at its ends. The stiffness K_s of this bare frame with a diagonal member of width w and pinned at its ends is given by the expression (Smith, 1966)

$$K_s = \frac{A+B+C}{C(A+B)}, \quad (3 16)$$

where

$$A = \frac{h \tan^2 \theta}{A_c E_f}, \quad B = \frac{d}{w t E_m \cos^2 \theta}, \quad \text{and } C = \frac{h^3 (3 I_b h + 2 I_c l)}{12 E_f I_c (6 I_b h + I_c l)} \quad (3 17)$$

In Eq (3.17), A is the lateral flexibility due to the axial deformation, B is the lateral flexibility due to diagonal strut, and C is the lateral flexibility due to flexural deformation of the frame. Further, A_c is the area of cross-section of column, d is the diagonal length of infill wall, w is the width of equivalent diagonal strut, and I_b is the moment of inertia of the top beam. For the frames at hand, $h=1,100$ mm, $l=2,000$ mm, $\theta=29^\circ$, $A_c=23,000$ mm², $E_f=32,000$ MPa, $d=2,059$ mm, $t=115$ mm, $E_m=3,160$ MPa, $I_b=7.67 \times 10^7$ mm⁴ and $I_c=7.67 \times 10^7$ mm⁴. A and C are determined from Eq (3.17) as 4.59×10^{-7} mm/N and 3.88×10^{-5} mm/N, respectively. To obtain the value of B from Eq (3.17), the effective width w of the diagonal strut is required. This is estimated as per the various models proposed in the literature, and discussed in section 1.2.1. The effective width w of the diagonal strut is obtained as 686 mm as per Holmes (1963), 330 mm as per Smith (1966), 210 mm as per Mainstone and Weeks (1970), 1,674 mm as per Hendry (1981) and 515 mm as per Paulay and Priestley (1992). Clearly, for a panel of size 1800 mm \times 1000 mm, an effective width of diagonal strut of 1,674 mm as per Hendry (1981) is unrealistic. Hence, this model is dropped henceforth. Thus, B is obtained from different models as 1.08×10^{-5} mm/N (Holmes, 1963), 2.24×10^{-5} mm/N (Smith, 1966), 3.52×10^{-5} mm/N (Mainstone and Weeks, 1970), and 1.44×10^{-5} mm/N (Paulay and Priestley, 1992). On substituting these values of A , B , C in Eq (3.16), the lateral stiffness of the infilled frame obtained as per different proposals of w , are shown in Table 3.1.

(ii) Shear Beam Model

A simple method for evaluation of the lateral stiffness of an infilled frame based on the shear beam model is available in literature (Fiorato *et al*, 1970). In the model, the infilled frame is taken as a composite cantilever beam made of masonry panel and RC columns, and the lateral stiffness is given by

$$K_b = \frac{K_{sh}K_f}{K_{sh} + K_f}, \quad (3.18)$$

where K_{sh} , the shear stiffness, and K_f , the flexural stiffness of the composite cantilever beam are given by

$$K_{sh} = \frac{A_w G_w}{h_w}, \text{ and} \quad (3.19)$$

$$K_f = \frac{3E_m I}{h^3} \quad (3.20)$$

In Eqs (3.19) and (3.20), A_w and G_w are the horizontal cross-sectional area and shear modulus of the infill, respectively. And, I is the moment of inertia of the composite beam, calculated using modular ratio $m = \frac{E_f}{E_m}$ of the frame-masonry composite section. For the frame at hand, the equivalent width of the masonry in the composite beam is taken as 115 mm and that of the column is taken as $m \times 115$ mm. Also, $m = 10.13$, $h_w = 1,000$ mm, and $A_w = 1800 \times 115 = 2.07 \times 10^5$ mm². Assuming Poisson's ratio ν as 0.25 and G_w as 1,260 MPa, K_{sh} and K_f are obtained as 262 kN/mm and 2,869 kN/mm. Thus, from Eq.(3.18), the value of K_b is obtained as 240.1 kN/mm.

(iii) Finite Element Method

Lateral stiffness of the infilled frame is obtained using standard FEM package, namely SAP2000 (Habibullah, 1995). The beams and columns are discretized into a total of 40 frame elements and the infill is discretized into 64 elements (Figure 3.3). The frames, tested in the laboratory are fastened by means of two steel girders, each made of two I-sections, and four anchor bolts. The steel girders are located at a distance of 150 mm away from the outer faces of the columns. Loose material is filled into any spaces between the bottom beam and strong floor. It is difficult to model this support condition exactly

Hence, two alternate idealisations are employed. In the first (Figure 3.3a), it was assumed that the two nodes in the bottom beam at the location of actual supports are fixed against translations and rotations (*i.e.*, fixed-fixed condition). In the second (Figure 3.3b), one node is assumed to be restrained against translations but free to rotate (*i.e.*, hinge support) and the other node restrained only against vertical translation but free to translate laterally and rotate (*i.e.*, roller support).

The stiffness of the infilled frame from the above two models is obtained as 207 kN/mm and 190 kN/mm, respectively. The second idealisation model appears to be more reasonable since the depth of the bottom beam is greater than the width of steel girders used for fastening the specimen to the strong floor.

(iv) Comparison

From the stiffness computed as per various models, the shear-beam model gives stiffness on the higher side. This overestimation of stiffness is attributed to the perfect bond assumed at the frame-panel interface unlike in practice (Schuller *et al.*, 1994b). The stiffness computed by SAP2000, should be lower than the stiffness computed by shear beam model, owing to the limited connectivity between the frame members and infill wall at nine nodes along the length of each member. However, the accuracy of these computations also depends upon how well the modulus of elasticity of brick masonry is estimated. The stiffness from the different models by the diagonal strut approach vary owing to the assumption behind the derivation of the expressions for width of equivalent diagonal strut. From Table 3.1, this variation is as much as the estimate as per Mainstone and Weeks, 1970.

3.2.2 Frame Without Infill (MRF 2)

(a) Strength

The strength of bare frame due to flexural failure of columns, is based on formation of plastic moment hinges at the ends of the columns as discussed in section 3.2.1. The ultimate moment capacity calculations given in section 3.2.1 are repeated for the bare frame with $f_{ck}=29.9$ MPa. The ultimate lateral strength of the frame is obtained as 36.4 kN. Again, the shear capacity of the two columns is obtained as 94.4 kN, which is larger than the strength of the bare frame obtained from flexural failure.

(b) Stiffness

The stiffness of bare frame also is obtained using SAP2000. The frame members are modeled with 40 frame elements of concrete (Figure 3.4). Again, two idealisations with different boundary conditions (*i.e.*, fixed-fixed and hinge-roller) were analyzed (Figure 3.4a and b). The stiffness obtained for these models is 15.5 kN/mm, and 15.3 kN/mm, respectively.

3.3 Experimental Observations On Frames

3.3.1 Frame With Infill (MRF 1)

The first visual influence of loading on the frame is seen in the form of separation of frame and infill at the top corner of the far column (from the loading) along the tension diagonal at a load of 56.65 kN (lateral displacement $\Delta=0.86$ mm, storey drift $\delta=0.08\%$) in the 6th cycle. In the 7th cycle, the separation of infill and frame is observed at the base of far column at a load of -48.75 kN ($\Delta=-1.06$ mm, $\delta=0.096\%$). In the same cycle, a crack is observed in the beam-column joint atop the near column (from the loading) at a load of 73.3 kN ($\Delta=1.31$ mm, $\delta=0.12\%$), owing to severe stress concentration at the collar plate.

In 8th cycle, wide separation between frame and infill is observed at the top corner that separated in the 6th cycle, this is noted at a lateral load of 70.1 kN ($\Delta=1.70$ mm, $\delta=0.15\%$). A small crack is observed in the beam-column joint atop the far column at a lateral load of -64.22 kN ($\Delta=-1.56$ mm, $\delta=0.14\%$) in the 10th cycle. In the same cycle, at load of 89.4 kN ($\Delta=3.06$ mm, $\delta=0.28\%$) the second layer of bricks from the top started sliding over the third layer of bricks. Indeed, this is the ultimate load for the MRF 1. Considerable slip between the horizontal layers of bricks is observed in the 11th cycle, in addition to spalling of mortar from the different layers of bricks and widening of the separation between frame and infill. The flexural cracks in the columns are developed as the infill is highly deformable owing to sliding of brick layers. The beam-column joints on the top showed increased cracking.

During the 12th cycle at a lateral load of 79.02 kN ($\Delta=3.58$ mm, $\delta=0.32\%$), the contact of the frame and the infill is observed to be only marginal along the height of the brick masonry. In the 13th cycle ($\Delta=5.89$ mm, $\delta=0.53\%$), the seventh layer of bricks from the top also began sliding. During the 15th cycle ($\Delta=5.98$ mm, $\delta=0.54\%$) and the 16th cycle ($\Delta=8.46$ mm, $\delta=0.76\%$), sliding is observed in many more layers of bricks. In these cycles, inclined cracks starting from the frame corners are also formed in bricks, which joined the sliding cracks in different layers. These inclined cracks increased throughout the infill. In the 23rd cycle ($\Delta=\pm 23.5$ mm, $\delta=2.14\%$), the flexural cracks at the base of the columns widened. In the 25th cycle ($\delta=3.48\%$), the maximum range of the LVDTs used at the top and mid-height of frame is exhausted. The LVDTs are disconnected and the test is continued until the snapping of reinforcement bars is heard. A view of frame after failure is shown in Figure 3.5.

3.3.2 Frame Without Infill (MRF 2)

In MRF 1, the beam-column joints experienced cracking owing to a local stress concentration due to small collar plates of size 200×150×20 mm. To prevent this in MRF 2, the size of collar plates is increased to 200×200×35 mm. Interestingly, flexural cracks were initiated in the two columns at the face of the top and bottom beam in the 4th cycle at the lateral loads of 11.31 kN (Δ = 1.44 mm, δ = 0.13%) and at -13.70 kN (Δ = -1.30 mm, δ = 0.12%). As the load is increased, these cracks run through the cross-section of the column and their widths increase.

In 10th cycle at a lateral load of 22.12 kN (Δ = 3.43 mm, δ = 0.31%) and at a lateral load of -22.65 kN (Δ = -2.46 mm, δ = 0.22%) flexural cracks at different sections of columns are observed. The cracking in columns increases after the beam-column joints cracks on continued loading due to shear failure of joint. In cycles 19 and 20, the spalling of cover concrete at the ends of the beams is observed owing to a longitudinal separation of the main bars from the beam. The crushing of concrete at the column ends and separation of the column from the base beam is observed, which increases with the load. The ultimate lateral load is observed as 43.5 kN (Δ = 23.3 mm, δ = 2.1%) in the 25th cycle. A view of the frame after failure is shown in Figure 3.6. The overall failure pattern showed significant cracking and damage in the columns with some spalling of cover concrete at the ends of the beam.

3.4 Discussion of Experimental Results

3.4.1 Load Displacement Response

The overall behaviour of the RC frame under cyclic loading is reflected by the hysteretic load-displacement response. The cyclic load-displacement hysteresis curves of the two specimens tested are shown in Figures 3.7a and 3.7b. The load is recorded from load

cell of the actuator and the net displacement is obtained from (LVDT 1-LVDT 4). (i.e., the displacement at the top beam level after accounting for the slip at the base, if any) The hysteresis loops for MRF 1 are much larger with increased strength and stiffness as compared to those for MRF 2. Both specimens experience some pinching, which is a characteristic of the reinforced concrete specimen and is recognised by the narrow width of the hysteresis loops near mid-cycles. Pinching is more in MRF 1 as compared to MRF 2, owing to higher level of inelasticity due to slip and cracking in MRF 1. This observation seems reasonable in the infilled frame wherein the infill brick masonry also participates with the frame members in resisting the lateral load and undergoes significant sliding between the brick layers.

3.4.2 Strength

The ultimate lateral load carrying capacity of MRF 1 is experimentally observed to be 89.4 kN, and its analytical estimate is 69.1 kN considering sliding shear failure of masonry plus flexural failure of columns. For MRF 2, the experimental lateral load capacity is obtained as 43.5 kN, and its analytical estimate is 36.4 kN. The experimental results show that in the present case the infilled frame has about two times the lateral load carrying capacity of the bare frame, the difference being attributed to the participation of the infills.

The same displacement excursions are repeated three times at each level to study the strength deterioration under repeated loading. The loss of strength during repeat cycles is seen from the load-displacement curve shown in Figure 3.7. The strength deterioration is measured as the loss of strength, expressed as a percentage, under repeated cyclic displacement excursions of the same amplitude with respect to the strength in the first of the three cycles. For the two specimen at hand, the strength deterioration for different

displacement levels is shown in Table 3.2. These results show that the strength deterioration is significantly higher in the second repeat cycle, particularly for MRF 1. This suggests that the loops do not stabilize, implying continued increase in inelasticity under repeated loading with same displacement excursions. This is also evident during the experiment, wherein in MRF 1 the cement mortar between the brick layers is noticed to grind and come out under cyclic loading.

Further, the strength deterioration is much smaller in MRF 2 in comparison to that in MRF 1. Since MRF 2 is a bare frame, the inelasticity is concentrated only at the ends of the column members. In MRF 1, the inelasticity is widespread in the infill wall panel, and near the ultimate load, it is also distributed along the length of the column members and not just at their ends. Thus, the reduced strength deterioration in MRF 2 is well explained from the localized damage pattern in it.

3.4.3 Stiffness

The initial stiffnesses of MRF 1 and MRF 2 are obtained from the slope of the line joining the origin with the first point on the load-displacement curve in the first cycle of loading, as 166.0 kN/mm for MRF 1 and 9.1 kN/mm for MRF 2. Thus, the initial stiffness of the infilled frame is about 18 times that of the corresponding bare frame. An average cycle stiffness is used to study the stiffness degradation in MRF 1 and MRF 2. The average cycle stiffness has been defined in literature in different ways. One definition takes it as the slope of the tangent at 75% of the maximum load for that cycle (Choubey, 1990; Pillai, 1995). In another definition, it is taken as the ratio of maximum load attained in a cycle and the displacement at that load (Raffaello and Wight, 1992). A third definition considers the secant stiffness which is the slope of a line connecting the extreme points of a small amplitude displacement cycle in which the peak load is about

50% of the maximum lateral resistance (Schuller *et al*, 1994b) In this study, the average cycle stiffness of a hysteresis loop is taken as the slope of the line joining the two extremities of the loop (Figure 3.8) The average cycle stiffness for MRF 1 and MRF 2 are presented in Table 3.3 as a function of the displacement excursion level. In general, a decrease in stiffness is observed with an increase in the displacement excursion level The degradation in the average cycle stiffness during the repeat cycles is measured as a percentage of that in the first of the three cycles with the same displacement excursion levels. The degradation in stiffness with displacement excursion level is very fast in MRF 1 as compared to MRF 2. In case of the infilled frame, both infill and frame jointly resist the load But after cracking of the infill, the stiffness offered by the infill is drastically reduced. Since no infills are present in MRF 2, such a drastic drop in stiffness is not seen in MRF 2.

3.4.4 Ductility

Ductility of a structure is its ability to undergo deformations beyond the yield deformation under cyclic loading. The load-deformation curves obtained as an envelope of the cyclic hysteresis loops, are shown in Figure 3.9. To obtain the yield displacements, these curves are idealised as elastic-perfectly plastic curves. The stiffness at 75% of the ultimate load of the actual curve is taken as the stiffness of the idealised curve, and ultimate strength of the idealised and actual curves are the same The yield displacement Δ_y of these curves is calculated as 1.49 mm for MRF 1 and 8.60 mm for MRF 2. A displacement ductility factor is defined as the ratio of the displacement excursion in the loading or unloading path (as explained in Figure 3.8) and the yield displacement. The displacement ductility factor as defined above is calculated for MRF 1 and MRF 2, and shown in Table 3.4. Further, a cumulative ductility factor is defined to compare ductilities

of MRF 1 and MRF 2. The cumulative ductility factor of a frame is taken as the sum of the displacement ductility factor in all cycles upto the cycle under consideration (Choubey, 1990, Pillai, 1995). Cumulative ductility factor upto final cycle for the infilled frame shows that it is about 11 times that of the bare frame. The higher ductility of MRF 1 is attributed to its smaller yield displacement and higher stiffness.

3.4.5 Energy Dissipation Capacity

The energy dissipation capacity of the frames in each cycle of loading is estimated from the area within the hysteresis loops of the load-displacement curve for that cycle. The cumulative of the energy dissipated during all the cycles is a measure of the total energy dissipation capacity of the frame. This cumulative energy is compared in both absolute and relative sense in Figures 3.10a and 3.10b. In Figure 3.10b, the cumulative energy is normalised with the elastic energy dissipated by the frame during loading upto yield assuming an idealised elastic-perfectly plastic behavior. The energy dissipation capacity of the infilled frame is much larger than that of the bare frame. This seems reasonable owing to much more extensive levels of inelasticity in the infilled frame.

3.4.6 Strain

The axial strains in the longitudinal reinforcement bars are monitored to identify yielding and slippage in them under cyclic loading. The longitudinal bars and the locations along it where the strains are measured are shown in Figures 2.7 and 2.8. However, data was available only from the strain gauges whose numbers are boxed in these figures. These strain-displacement excursion plots for the different bars in MRF 1 and MRF 2 are shown

in Figures 3.11 and 3.12, respectively. The cyclic variation of stress around the bar from compression to tension (or *vice-versa*) results in a strain pattern which suggests that the compressive stress is transferred through both the bars and the core concrete (Raffaello and Wight, 1992). The yield strain for the bars is around 2000 microstrain. In MRF 1, the strain gauges 3 and 19 at the ends of the column show yielding at a lateral load of about 75 kN (Figures 3.11d and 3.11e). However, these were the strain gauges which show yield much earlier than the others. The load-displacement envelope of MRF 1 (Figure 3.9) shows a sudden non-linearity at a lateral load of 73.36 kN. So, this may be considered as the load at the first yield for MRF 1. The strain gauges 1, 21, 9 and 20 in the top beam show small amount of slippage at initial cycles. For this reason, strain gauges 1, 21 and 20 may not have yielded. However, strain gauge 9 is seen to yield at a lateral load of about 50 kN (Figures 3.11i, 3.11j, 3.11h and 3.11g). So, based on the general behaviour of strain gauges in the top beam, it may be said that no yield is reached in the beam. The strain gauges in the columns (*i.e.*, strain gauges 2, 14 and 17) show yielding at a lateral load of about 60 kN (Figures 3.11f, 3.11b and 3.11a) in the 23rd cycle.

In MRF 2, the yielding strain was first approached at the bottom section of columns noticed through strain gauges 14, 23 and 24 at a lateral load of 30 kN (Figures 3.12c, 3.12d and 3.12f). In fact, these strain gauges yielded much before the other strain gauges. From load-displacement envelope of MRF 2 (Figure 3.9), a major non linearity is observed at a lateral load of 26.1 kN. So, this may be taken as the load at the first yield for the MRF 2. The strain gauges 10, 12, 15 and 18 in the beam show large slip. As in MRF 1, the strain gauges 10, 15 and 18 did not yield. However, strain gauge 12 yielded at a load of 30 kN in the 24th cycle (Figures 3.12i, 3.12g, 3.12h and 3.12j). So, from the general behaviour, it may be interpreted that no yield is observed in the beam. The yielding in strain gauges 17 and 19 in the column is observed at lateral load of 30-35 kN

in the 23rd cycle (Figures 3.12a and 3.12b). Considerable amount of slip is also observed in the column longitudinal bars.

From the above description, the initial cracks in infilled frame observed at the both ends of the columns are convincing. In the bare frame, flexural cracks were first observed at the bottom of the column, and the strain gauges at these locations also reflect the same.

3.5 Concluding Remarks

The following salient issues arise out of this experimental study:

- (1) The analytical estimates of the stiffness and strength of infill frames depend largely on the modulus of elasticity E_m of the brick masonry. Empirical expressions need to be developed for E_m of brick masonry used in India.
- (2) The separation of infill panel from frame occurs first, and only then cracks are developed in the infill or frame. This suggests that if the quality of contact, workmanship and material are improved, then the separation of the frame and infill wall panel may be delayed to occur at larger loads, the cracks in infill or frame will develop only subsequently.
- (3) The current method of using a collar arrangement around the top beam to apply cyclic displacement history causes local concentration of stresses. A mechanism needs to be developed to apply the loading without causing unrealistic load conditions at the frame corners.
- (4) In the infilled frame, cracks in the wall panel are of two types, namely (a) inclined cracks, and (b) horizontal sliding cracks connected to each other by inclined cracks. Increased slip occurs along the bed joints with increase in crushing and degradation of mortar. While the lateral resistance of the infilled frame seems to be governed mainly

by sliding failure of the wall panel along bed joints followed by flexural failure of frame, the experimental strength of specimen is 25% larger than the sum of sliding resistance of the wall panel and flexural resistance of the bare frame estimated analytically. The disparity raises question on the capability of the analytical models to accurately predict the strengths, and more importantly on the contribution of the diagonal strut to the observed failure mechanism.

- (5) From the analytical stiffness estimates based on various models for infilled frames, the shear-beam model is generally known to overestimate the stiffness, owing to the assumption of a perfect bond at the frame and infill interface as well as between the brick units, which is quite unlikely in real practice (Schuller *et al*, 1994b). On the other hand, the stiffness computed by SAP2000, is found to give values lower than the stiffness computed by shear-beam model. This is attributed to the connectivity between frame and infill at few discrete points. The stiffness computed by the diagonal strut approach varies depending on the approach adopted. For the frame at hand, the proposal of Mainstone and Weeks, 1970 gives the smallest value and that of Holmes, 1963 gives the largest value.
- (6) The stiffness of both frames degrades when subjected to cyclic loading, but it is much higher in the infilled frame. The stiffness loss is attributed to cracking in infill and frame and to the yielding of reinforcement. The pinched hysteresis loops in the infilled frame for the cycles of larger displacement excursions beyond yield is a reflection of the large amount of sliding in the infill panel.
- (7) The decrease in the average cycle stiffness for the infilled frame is rather sharp once the infill cracks. This reiterates that the stiffness contribution of the infill may be many times that of the bare frame alone.

-
- (8) From the cumulative ductility factors (upto ultimate load cycles) for the two frames, the infilled frame MRF 1 seems more ductile than the bare frame. This is due to lesser yield displacement and higher stiffness of the infilled frame.
- (9) The infilled frame has better energy dissipation capacity than the bare frame.
- (10) The strength deterioration increases with increase in displacement excursion level. The loss in strength is also attributed to the cracking in infill and frame and to the yielding of the reinforcing steel. The rate of increase in strength deterioration is more rapid in the infilled frame owing to significant inelasticity in the infill.
- (11) The frame behaviour shows initial cracks either at beam-column junctions or at bottom of columns. This expects that steel at these sections should yield, which is observed through the load-strain curves of the bars.
- (12) From the extensive sliding in the infill frame, the size of the bricks used seems to be large in comparison with the cross-section size of the frame members and the size of the infill panel. Smaller brick sizes may be considered in future studies.

● ● ●

Chapter 4

SUMMARY AND CONCLUSIONS

4.1 Summary

The main objective of this work was to study the behaviour of reinforced concrete frames with and without brick masonry infills under pseudo-static cyclic lateral loads. This study attempted to provide an improved understanding of the mechanism of cyclic behaviour of unreinforced masonry filled RC frames. For this purpose, two frames one infilled and the other bare, were studied. Both the frames were one-bay single-storey portal frames. Cyclic lateral load was applied horizontally at the top beam level in displacement control. No vertical loads or out-of-plane loads were applied on the frame. The properties of the various materials, which are used for construction of frame and infill wall were experimentally obtained. The analytical estimates of strength and stiffness of infilled frames were obtained using models available in literature. These were compared with the experimentally measured quantities, and found to be in good agreement.

4.2 Conclusions

The salient conclusions derived from the relative performance of the infilled and the corresponding bare frames of this study are

- (1) The lateral load capacity of the infilled frame is about two times that of the bare frame.
- (2) The initial stiffness of infilled frame is about 18.2 times that of the bare frame. The diagonal strut analogy concept seems to underestimate the stiffness.

- (3) The infilled frame studied is more ductile than the bare frame. The cumulative ductility factor of infilled frame is about 11 times that of the corresponding bare frame studied.
- (4) The infilled frame studied has higher energy dissipation capacity than the corresponding bare frame. The cumulative energy dissipated in the infilled frame is about 5 times that in the bare frame.
- (5) The stiffness of the infilled frame is observed to decrease upto 95% of its initial stiffness with increase in displacement excursion level of upto 16 times the yield displacement. However, this decrease is only about 30% of its initial stiffness in the bare frame where the displacement excursion of about 3 times the yield displacement is applied on it.

The cracking in the frame or in the infill occurs only after the separation of infill and frame has taken place. Hence, it seems that the quality of contact (e.g., mortar strength) between frame and infill may influence the strength, stiffness and cyclic behaviour of the frame. The behaviour of the infilled frame seems better than that of the bare frame in all aspects. In the design of infilled RC frames, the presence of infills should be recognised. They are not non-structural elements. A procedure to bring the infills into design process is required.

4.2 Scope of Further Work

This investigation is only a small effort and a vast scope of research exists in this field. Some points that arise from this study for future considerations are noted below:

- (1) A study of infilled frames with openings may provide valuable information.
- (2) In present study, regular size bricks are used in the infill wall masonry, but the frame size is a 1:2:7 reduced scale model of practical frames. Reduced brick sizes may be attempted. This may permit diagonal strut failure of infill panel.

-
- (3) The application of the displacement history through the collar arrangement at the top beam needs to be revised to avoid local concentration of stress in the already critical beam-column junctions. A slab-beam sub-assembly may be considered at the top beam level to facilitate the application of lateral loads.

• • •

REFERENCES

- Achintya, Dayaratnam,P , and Jain,S K , 1991, "Behaviour of brick infilled reinforced concrete frame under lateral load," *Indian Concrete Journal*, Vol 65, No 9, pp 453-457
- Altin,S , Ersoy,U , and Tankut,T , 1992, "Hysterstic response of reinforced concrete infilled frames," *Journal of Structural Engineering*, ASCE, Vol.118, pp 2133-2149
- Choubey,U B , 1990, "Behaviour of infilled frames under cyclic loads," **Ph.D. Thesis**, Department of Civil Engineering, Indian Institute of Technology Delhi, India
- Dayaratnam,P , 1987, **Brick and Reinforced Brick Structures**, Oxford and IBH Publishing Co Pvt. Ltd , India.
- Dhanasekar,M., and Page,A W., 1986, "The influence of brick masonry infill properties on the behaviour of infilled frames," *Proceedings of the Institution of Civil Engineers*, UK, Vol.81, pp 593-605.
- Drysdale,R G., Hamid,A.A., and Baker,L R., 1993, **Masonry Structures-Behaviour and Design**, Prentice Hall Inc. , New Jersey.
- Fiorato,A.E., Sozen,M.A., and Gamble,W L., 1970, "An investigation of the interaction of reinforced concrete frames with masonry filler walls," Technical Report No. UILU-ENG 70-100, University of Illinois, Urbana-Champaign, IL.
- Gavrilovic,P., and Sendova,V., 1992, "Experimental and analytical studies of infill walls in reinforced concrete structures-Review of seismic research results," *Proceedings of Tenth World Conference on Earthquake Engineering*, Spain, pp 153-155.
- Grimm,C.T., 1984, "Elastic modulus of clay brick masonry," *Proceedings of Reinforced and Prestressed Masonry Symposium*, University of Edinburgh, Scotland.
- Grimm,C.T., 1975, "Strength and related properties of brick masonry," *Journal of the Structural Division*, ASCE, Vol.107, pp 217-232
- Habibullah,A., 1995, **SAP2000-Integrated finite element analysis and design of structures**, CSI Inc. , California.
- Hamid,A.A., Ziab,G., and Nawany,O.E., 1987, "Modulus of elasticity of concrete block masonry," *Proceedings of Fourth North American Masonry Conference*, Los Angeles, USA
- Hart,G.C., 1989, "Seismic design of masonry structures," **Seismic Design Handbook**, Editor:F.Naeim, Van Nostrand Reinhold Company, USA.

Hendry,A , 1981, *Structural Brickwork*, MacMillan, UK

IS 456-1978, 1978, *Indian Standard Code of Practice for Plain and Reinforced Concrete*, Bureau of Indian Standards, New Delhi

IS 1893-1984, 1984, *Indian Standard Criteria for Earthquake Resistant Design of Structures*, Bureau of Indian Standards, New Delhi

Jain,S K , Saraf,V.K , and Mehrotra,B , 1997, "Experimental evaluation of fundamental period of reinforced concrete framed buildings with brick infills," *Journal of Structural Engineering*, SERC, Madras, Vol 23, pp 189-196

King,G.J.W , and Pandey,P C , 1978, "The analysis of infilled frames using finite elements," *Proceedings of the Institution of Civil Engineers*, UK, Vol.65, pp 749-760

Kodur,V.K R., Erki,M A., and Quenneville,J H P., 1995, "Seismic design and analysis of masonry-infilled frames," *Canada Journal of Civil Engineers*, Vol 22, pp 576-587.

Liauw,T.C., 1979, "Tests on multistorey infilled frames subjected to dynamic loading," *Journal of the American Concrete Institute*, Title No.76-26, pp 551-563

Liauw,T.C., and Lee,S.W., 1977, "On the behaviour and analysis of multistorey frames subjected to lateral loading," *Proceedings of the Institution of Civil Engineers*, UK, Vol.63, pp 641-656.

Mainstone,R.J., and Weeks,G.A., 1970, "The influence of bounding frames on the racking stiffness and strength of brick walls," *Proceedings of the Second International Brick Masonry Conference*, UK, pp 165-171.

Mallick,D V., and Severn,R.T , 1967, "The behaviour of infilled frames under static loading," *Proceedings of the Institution of Civil Engineers*, UK, Vol 38, pp 639-656.

Michailidis,C.N., Styliandis K.C. and Kapoos A.J., 1995, "Analytical modeling of masonry infilled reinforced concrete frames subjected to seismic loading," *Proceedings of Tenth European Conference on Earthquake Engineering*, pp 1519-1524

Nagar,A., 1995, "Modeling seismic response of unreinforced masonry infilled reinforced concrete moment resisting frame," M.Tech. Thesis, Department of Civil Engineering, Indian Institute of Technology Kanpur, India.

Paulay,T., and Priestley,M.J.N , 1992, *Seismic Design of Reinforced Concrete and Masonry Buildings*, Wiley Interscience Inc. , USA.

Pillai,E.B.P., 1995, "Influence of brick infill on multistorey, multibay reinforced concrete frames," Ph.D. Thesis, Civil Engineering Department, Coimbatore Institute of Technology, India.

- Pires,F , and Carvalho,E C , 1992, "The behaviour of infilled reinforced concrete frames under horizontal cyclic loading," **Proceedings of Tenth World Conference on Earthquake Engineering**, Spain, Vol 6, pp 3419-3421
- Raffaella,G.S , and Wight,J.K , 1992, "R/C eccentric beam-column connections subjected to earthquake-type loading," **Research Report UMCEE 92-18**, The University of Michigan, USA
- Schuller,M., Mehrabi,A.B , Noland,J L , and Shing,P B , 1994a, "Performance of masonry infilled reinforced concrete frames under in plane lateral loads: Experiments," **Proceedings of the NCEER Workshop on Seismic Response of Masonry Infills**, Technical Report NCEER-94-0004, pp 27-32
- Schuller,M., Mehrabi,A B., Noland,J L., and Shing,P B , 1994b, "Performance of masonry infilled reinforced concrete frames under in plane lateral loads," Report No CU/SR-94/6, **Structural Engineering and Structural Mechanics Series**, University of Colorado Boulder, USA
- Smith,B S , and Carter,C., 1969, "A method of analysis for infilled frames," **Proceedings of the Institution of Civil Engineers**, UK, Vol.44, pp 31-48.
- Smith,B S., 1967, "Methods for predicting the lateral stiffness and strength of multi-storey infilled frames" **Building Science**, Britain, Vol.2, pp 247-257.
- Smith,B.S , 1966, "Behaviour of square infilled frames," **Journal of the Structural Division**, ASCE, Vol 92, ST1, pp 381-403
- Smith,B.S., 1962, "Lateral stiffness of infilled frames," **Journal of the Structural Division**, ASCE, Vol.88, ST6, pp 183-199.
- Smolira,M., 1973, "Analysis of infilled shear walls," **Proceedings of the Institution of Civil Engineers**, UK, Vol.53, pp 895-912
- Vegro,P., and Verzeletti,G., 1996, "Effect of infills on global behaviour of reinforced concrete frames: Energy considerations on pseudodynamic tests," **Journal of Earthquake Engineering and Structural Dynamics**, Vol 25, pp 753-773
- Whitney,C S., Anderson,B.G , and Cohen,E., 1955, "Design of blast resistant construction for atomic exploits," **Journal of the American Concrete Institute**, Vol.51, pp 655-673.
- Zarnic,R., and Tomazevic,M., 1988, " An experimentally obtained method for evaluation of the behaviour of masonry infilled reinforced concrete frames," **Proceedings of Ninth World Conference on Earthquake Engineering**, Japan, Vol.6, pp 163-168.
- Zarnic,R., and Tomazevic,M , 1984, "The behaviour of masonry infilled reinforced concrete frame subjected to cyclic lateral loading," **Proceedings of Eighth World Conference on Earthquake Engineering**, USA, Vol.6, pp 863-870

Table 2 1 Quantities of materials used in MRF 1 and MRF 2

Frame	Number of Batches	Quantity per Batch (kg)				Water (litres)
		Cement	Sand	Aggregate		
				20 mm	12.5 mm	
MRF 1	4	36 9	67 9	91 6	39 3	19 2
MRF 2	4	36 9	67 9	91 6	39 3	19 2

Table 2 2 Properties of cement used in MRF 1 and MRF 2

Cement Property	Results
Standard Consistency	28%
Setting Time (a) Initial	180 minutes
(b) Final	250 minutes
Compressive Strength (a) At 3 days	21 5 MPa
(b) At 7 days	28 1 MPa

Table 2 3 Properties of the bricks used in the construction of the infill panel

Brick Property	Results	
Dimensions (mm)	L	224
	B	110
	H	67
Compressive Strength (MPa)	18 7	
Water Absorption (%)	15 3	

Table 2 4 Average cube compressive strength of cement mortar used in MRF 1.

Age	Mortar Compressive Strength (MPa)
3-days	4 7
7-days	7 7
14-days	11 4

Table 2 5 Average cube compressive strengths of concretes used in MRF 1 and MRF 2

Frame	Compressive Strength (MPa)				Age on day of test (days)
	28-day		On day of test		
	Sample	Average	Sample	Average	
MRF 1	30 61	31 5	40 11	40 1	118
	32 48		39.73		
	31.39		40 51		
MRF 2	30 82	29 9	40 78	39 4	183
	28 88		37 56		
	29 88		39 92		

Table 2.6 Tensile tests on steel reinforcement bars used in MRF 1 and MRF 2

<i>Bar Diameter (mm)</i>	<i>0.2% Proof Stress (MPa)</i>	<i>Ultimate Stress (MPa)</i>
10	417	494
12	478	591

Table 3.1 Analytical estimates and experimental values of stiffness and strength of MRF 1 and MRF 2

<i>Property</i>	<i>Analysis</i>			<i>Experiment</i>	
	<i>Model</i>	<i>MRF1</i>	<i>MRF2</i>	<i>MRF1</i>	<i>MRF2</i>
<i>Strength (kN)</i>	Tensile Failure of Column	236.9		89.4	43.5
	Sliding Shear Failure of Masonry	31.3			
	Compression Failure of Diagonal Strut	244.8			
	Flexural Failure of Columns	37.8	36.4		
	Expected Strength	69.1	36.4		
<i>Stiffness (kN/mm)</i>	Diagonal Strut Model			166.0	9.1
	Holmes (1963)	114.6	-		
	Smith (1966)	70.1	-		
	Mainstone and Weeks (1970)	53.8	-		
	Paulay and Priestley (1992)	93.1	-		
	Shear Beam Model				
	Fiorato <i>et al</i> (1970)	240.1	-		
	Finite Element Method	190.0	15.3		

Table 3 2 Strength deterioration in MRF 1 and MRF 2 as a percentage of strength in first of the three cycles

<i>Applied Displacement Excursion Level (mm)</i>	<i>MRF 1</i>			<i>MRF 2</i>		
	<i>Strength in First Cycle (kN)</i>	<i>Strength Deterioration (%)</i>		<i>Strength in First Cycle (kN)</i>	<i>Strength Deterioration (%)</i>	
		<i>Repeat Cycle 1</i>	<i>Repeat Cycle 2</i>		<i>Repeat Cycle 1</i>	<i>Repeat Cycle 2</i>
1	37 67	0 3	2 1	5 16	2 9	3 1
-1	23 65	0 4	2 3	7 21	2 6	2 9
2	59 33	4 7	5 6	11 39	3 2	3 6
-2	38 10	5 1	6 2	13 62	2 7	3 1
3	73 36	5 5	8 2	17 23	3 7	4 8
-3	48 40	6 3	9 5	18 45	3 2	4 2
4	-	-	-	20 49	4 5	8 8
-4	-	-	-	22 38	3 9	8 1
5	89 40	6 9	10 8	26 10	2 7	3 2
-5	73 50	7 5	10 9	25 90	2 2	2 6
7 5	86 71	9 7	15 3	33 53	3 4	5 9
-7 5	75 91	10 2	15 7	33 40	3 4	6 0
10	84 23	8 1	11 9	37 47	6 2	8 7
-10	80 75	9 4	12 6	37 15	5 5	6 2
15	86 55	11 7	16 7	41 40	7 7	10 2
-15	89 40	11 1	15 9	40 84	6 7	9 3
25	80 65	19 6	26 7	43 50	-	-
-25	86 75	19 10	25 9	-	-	-
40	64 09	36 20	-	-	-	-
-40	68 00	29 26	-	-	-	-

Table 3 3 Stiffness degradation in MRF 1 and MRF 2 as a percentage of average cycle stiffness in first cycle

Applied Displacement Excursion Level (mm)	MRF 1			MRF 2		
	Average Cycle Stiffness in First Cycle (kN/mm)	Stiffness Degradation (%)		Average Cycle Stiffness in First Cycle (kN/mm)	Stiffness Degradation (%)	
		Repeat Cycle 1	Repeat Cycle 2		Repeat Cycle 1	Repeat Cycle 2
±1	161.1	2.1	3.1	7.6	1.1	1.9
±2	95.4	3.2	11.2	7.5	1.7	2.8
±3	51.1	9.5	12.1	7.2	0.7	1.1
±4	-	-	-	7.0	4.8	8.4
±5	32.1	16.3	20.6	6.8	1.6	6.4
±7.5	16.4	12.2	16.5	5.6	0.9	5.7
±10	11.2	8.9	16.9	4.5	3.5	5.8
+15	7.5	16.1	26.3	3.2	2.8	3.8
±25	4.0	20.7	57.2	2.8	-	-
±40	1.5	39.3	-			

Table 3 4 . Ductility factor of MRF 1 and MRF 2 at different displacement excursion levels

Applied Displacement Excursion Level (mm)	MRF 1		MRF 2	
	Average Displacement Ductility Factor (Δ/Δ_y)		Average Displacement Ductility Factor (Δ/Δ_y)	
	Loading	Unloading	Loading	Unloading
±1	0.30	0.36	0.09	0.12
+2	0.85	0.58	0.17	0.23
±3	1.08	1.42	0.26	0.28
±4	-	-	0.31	0.39
+5	2.03	2.85	0.44	0.43
±7.5	3.82	4.94	0.68	0.72
±10	5.56	6.85	0.97	1.00
±15	9.10	10.24	1.37	1.70
+25	16.71	21.02	1.48	1.64
±40	22.14	25.30	-	-
Cumulative Ductility Factor	135.12		12.28	

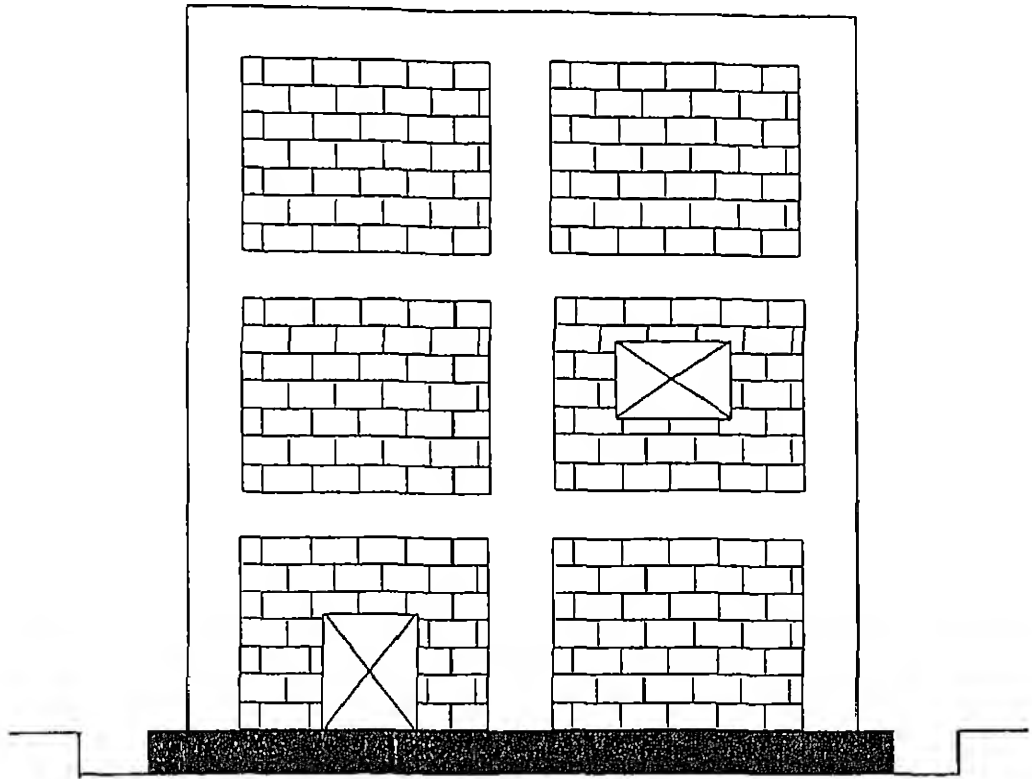


Figure 1.1: A typical planar RC moment resisting frame with unreinforced brick masonry infills

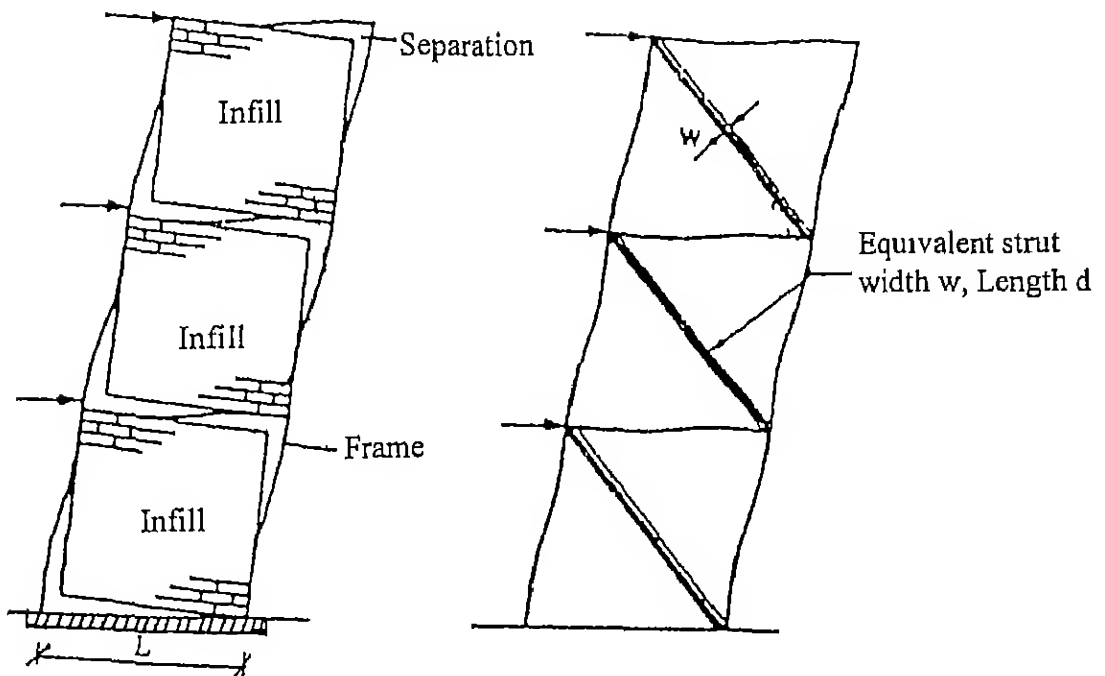


Figure 1.2: Separation between infill and RC frame member and strut action in infill (Drysdale *et al*, 1993)

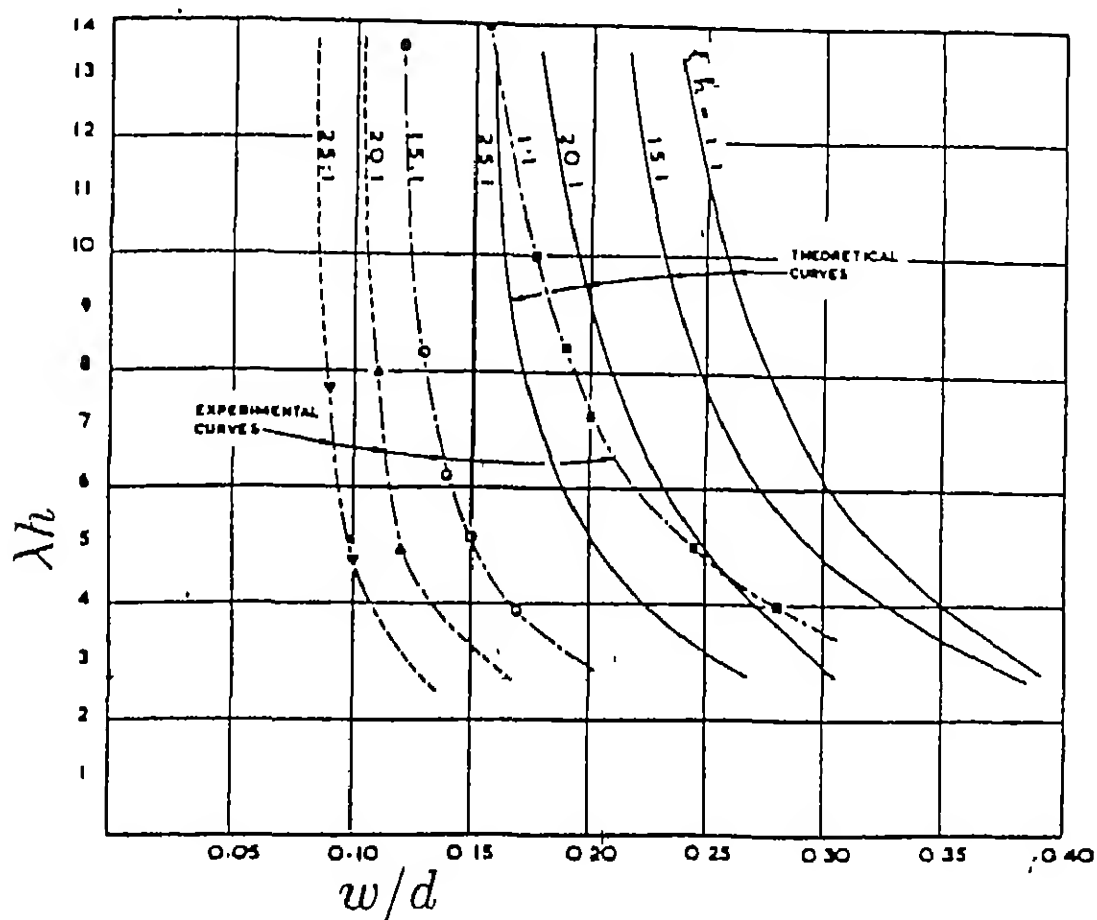


Figure 1.3: Effective width-vs-relative stiffness curves for frames of different aspect ratios (Smith, 1967).

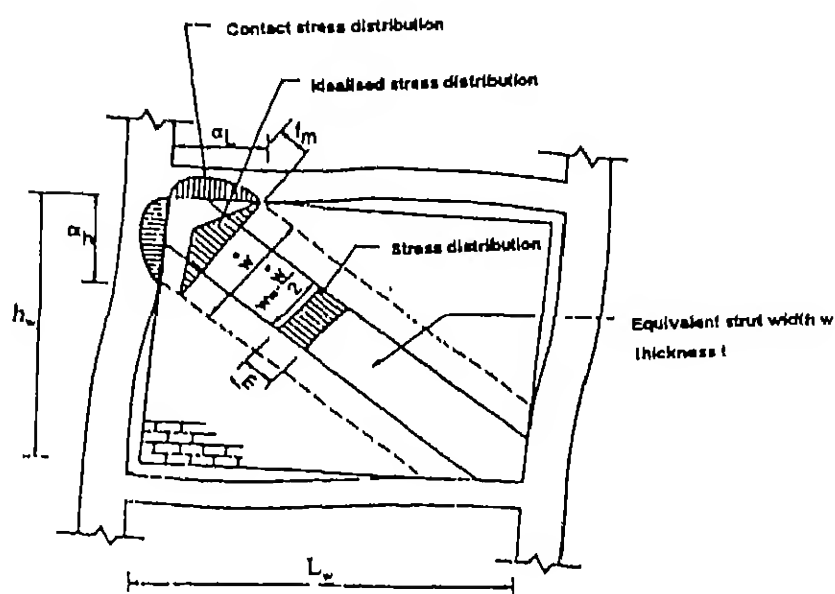
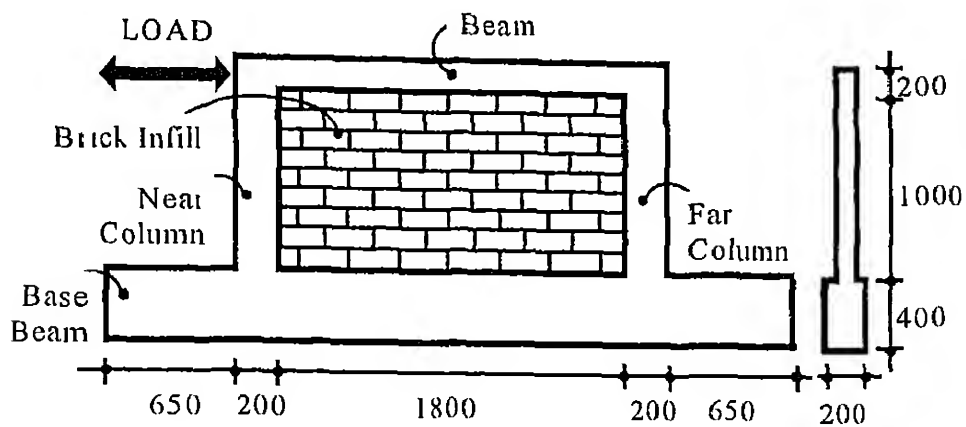
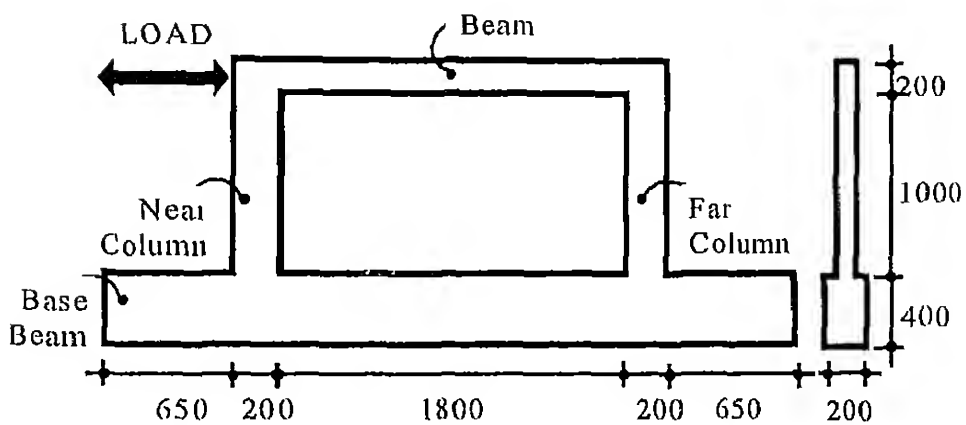


Figure 1.4: Diagonal strut action with notations (Drysdale *et al*, 1993)

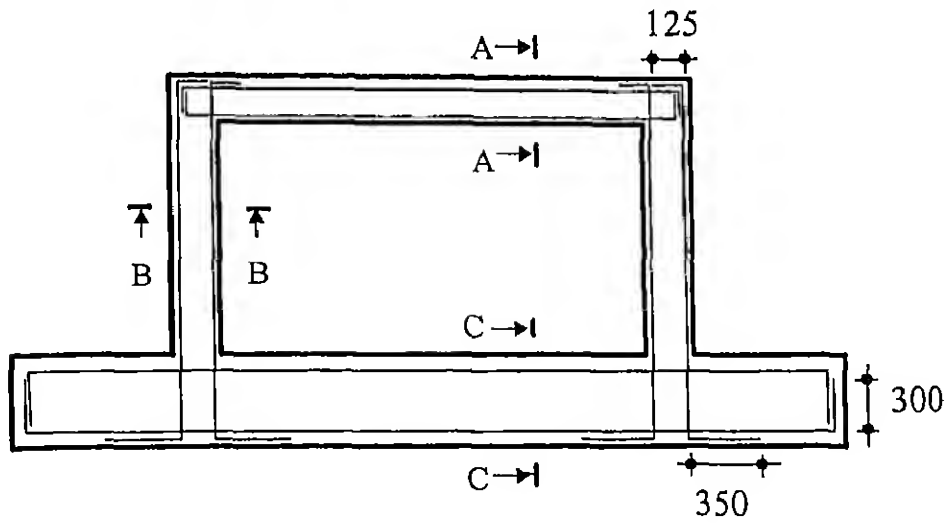


(a) MRF 1 (Infilled Frame)

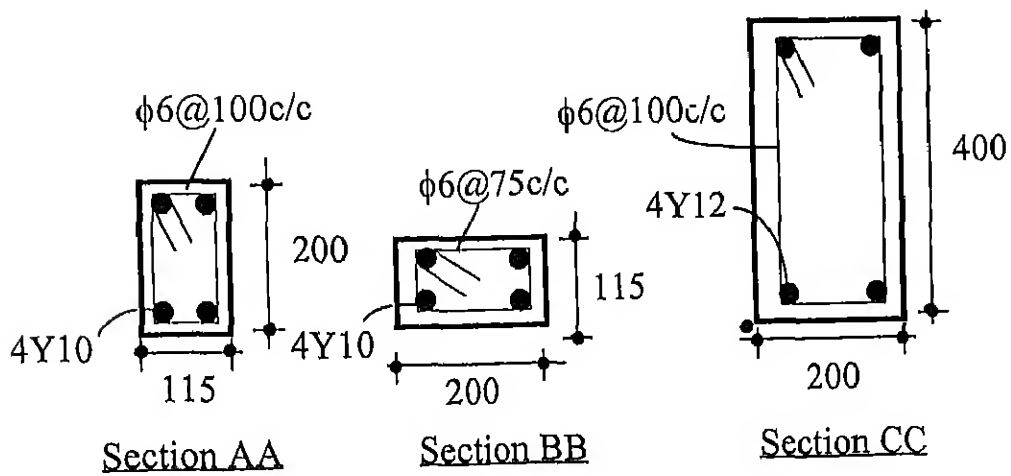


(b) MRF 2 (Bare Frame)

Figure 2.1: Geometry of the two frames tested. All dimensions are in mm.



(a) Sectional Elevation



(b) Cross-sections of Frame members

Figure 2.2: Details of reinforcement bars in MRF 1 and MRF 2. Grade of concrete used is M30, Clear cover to longitudinal reinforcement is 20 mm. All dimensions are in mm.

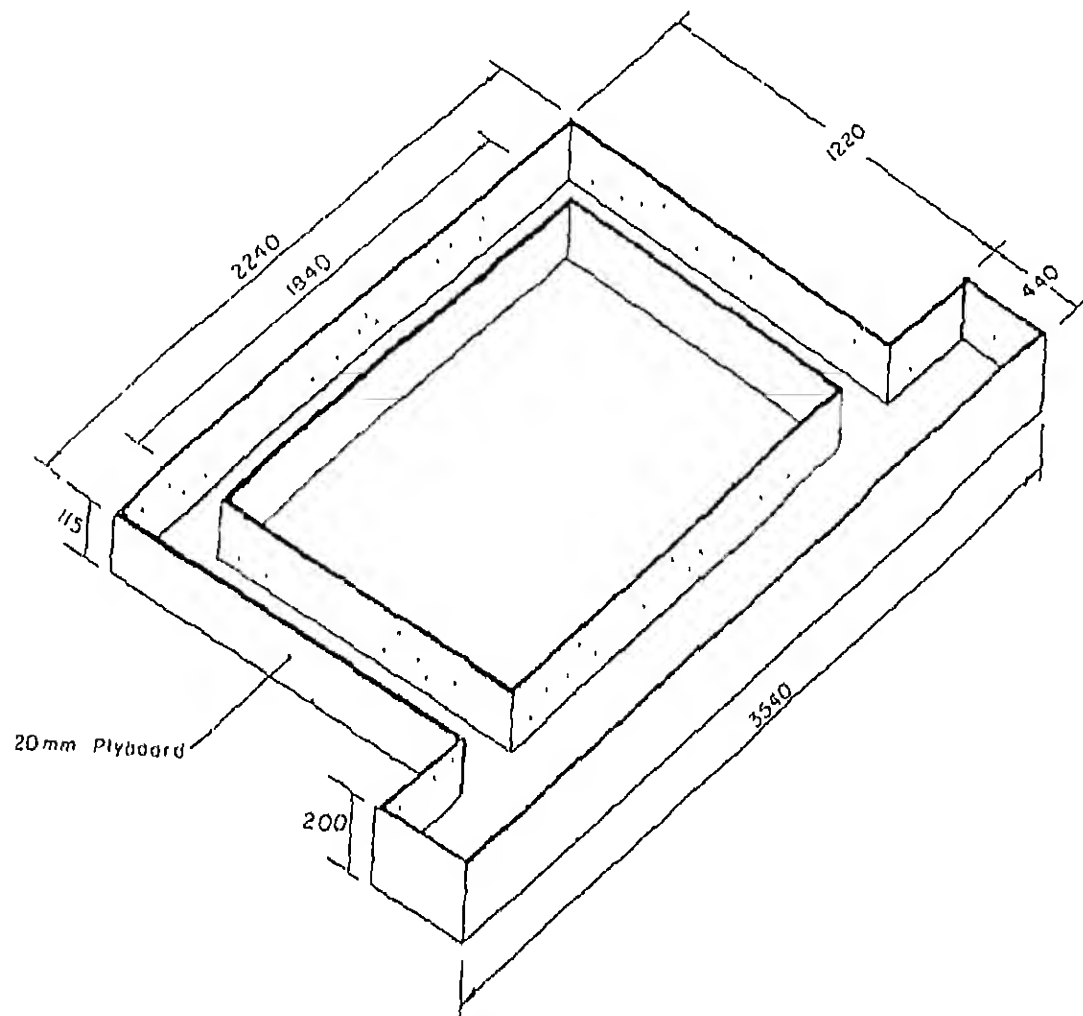


Figure 2.3: External dimensions of the wooden mould for casting the RC frame specimen. All dimensions are in mm.

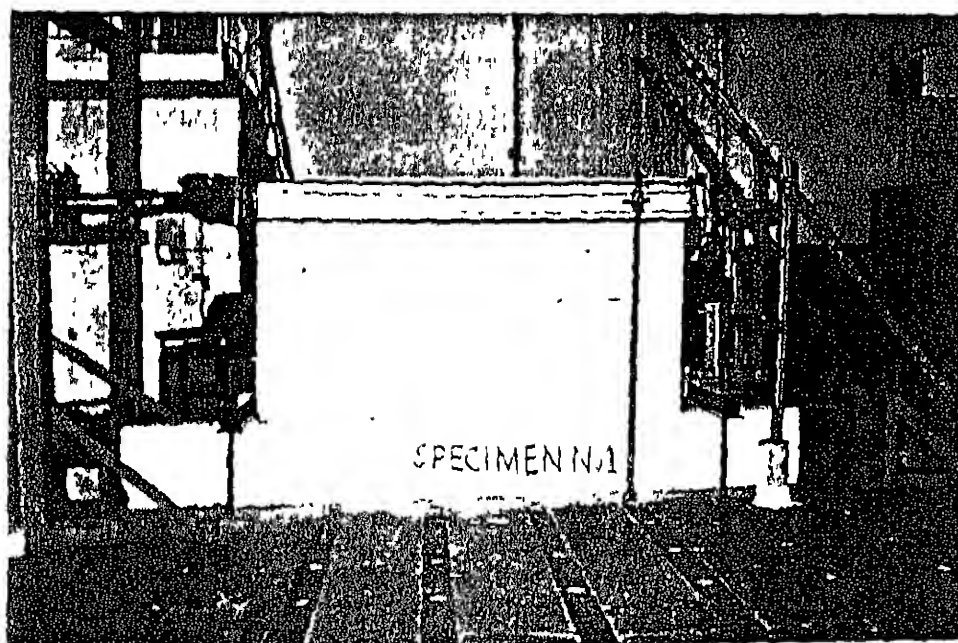


Figure 2.4: A view of the general arrangements of the specimen, the loading frame and the supports.

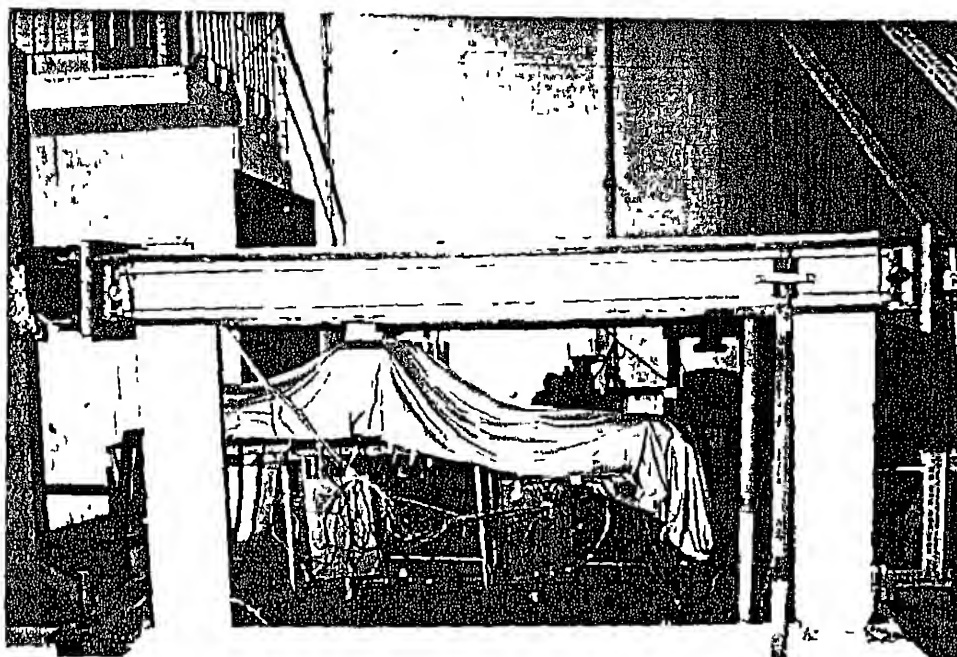


Figure 2.5: A closer-view of the collar around the frame at the beam level to apply reversed cyclic displacement history

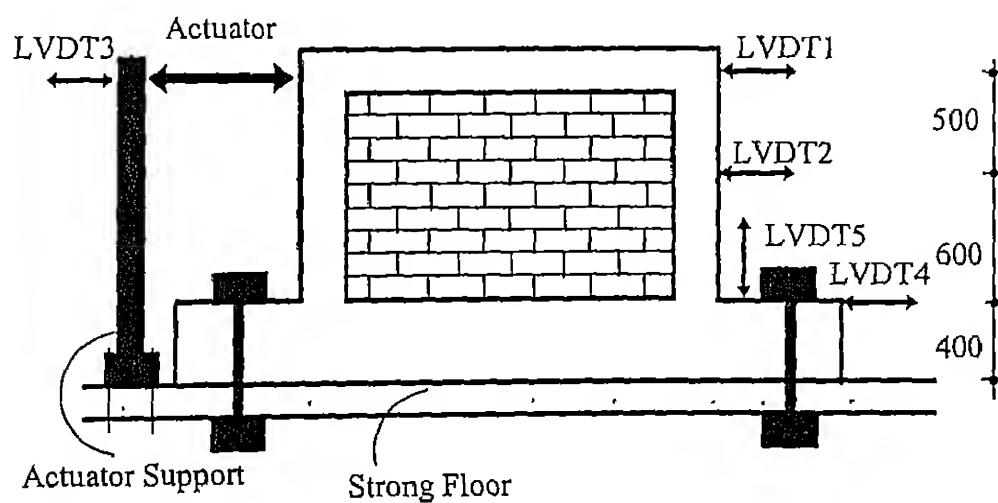
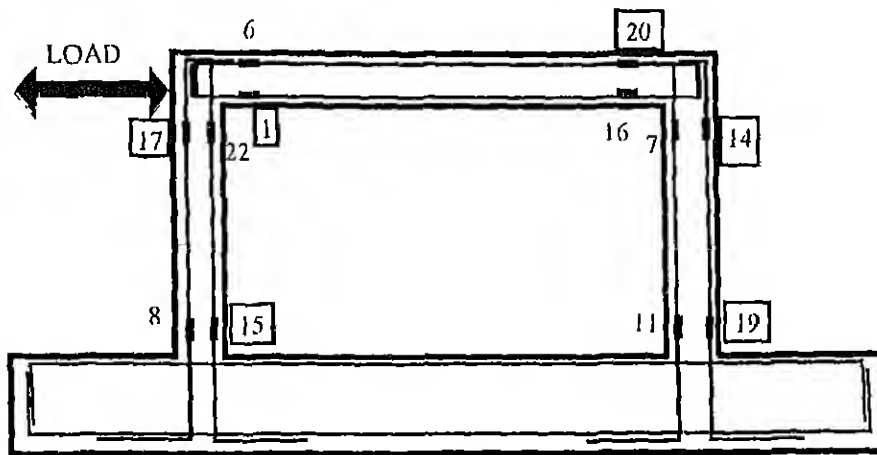
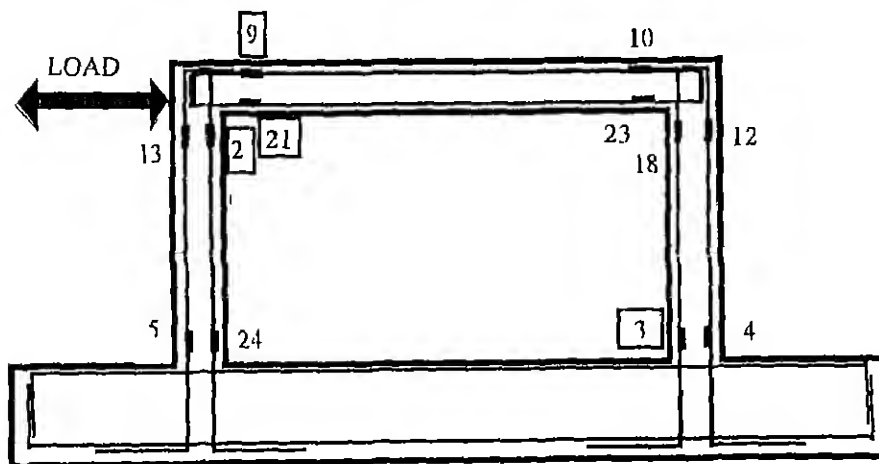


Figure 2.6. A schematic of the frame showing locations of LVDTs at which displacements are measured. All dimensions are in mm

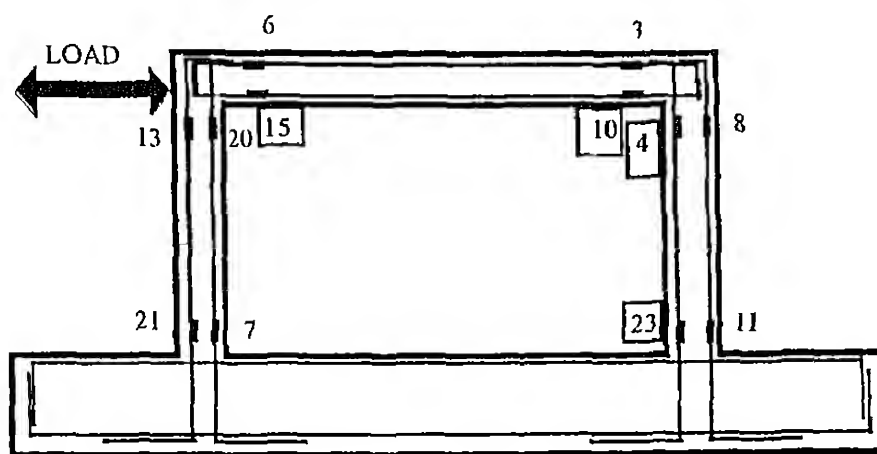


(a) Front Face

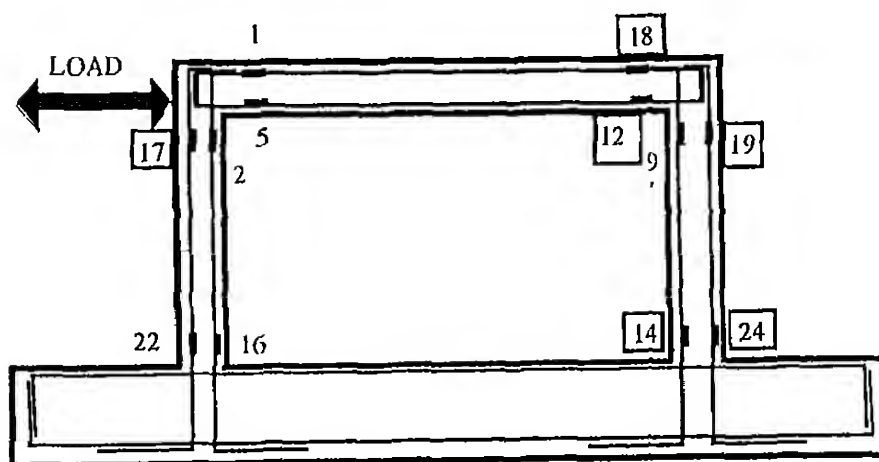


(b) Back Face

Figure 2.7: A schematic of the frame showing the locations of strain gauges pasted on the longitudinal reinforcement bars in MRF 1

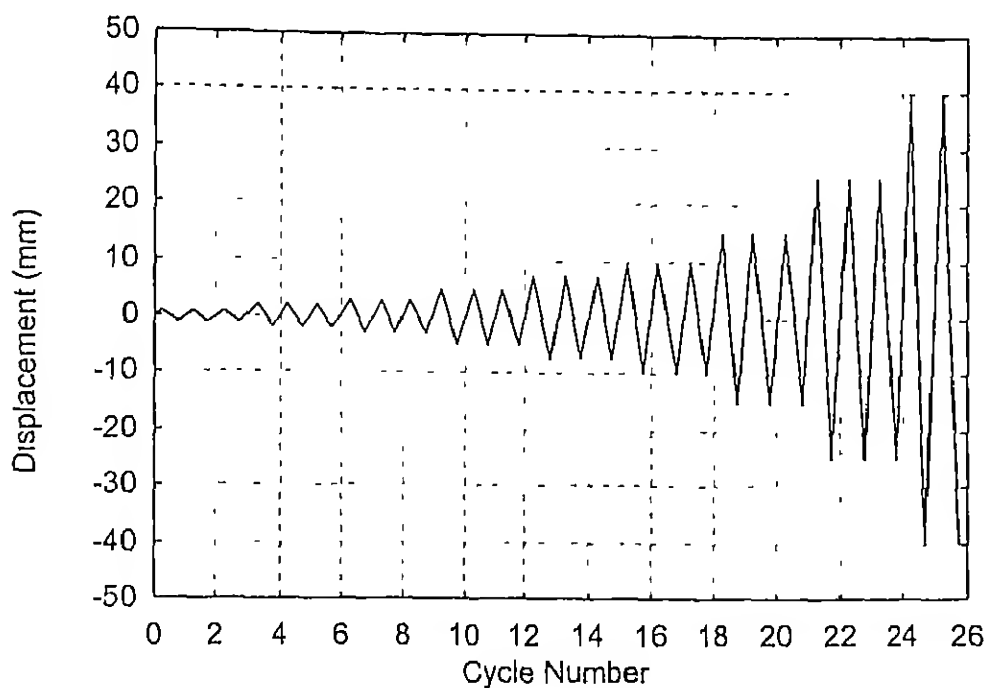


(a) Front Face

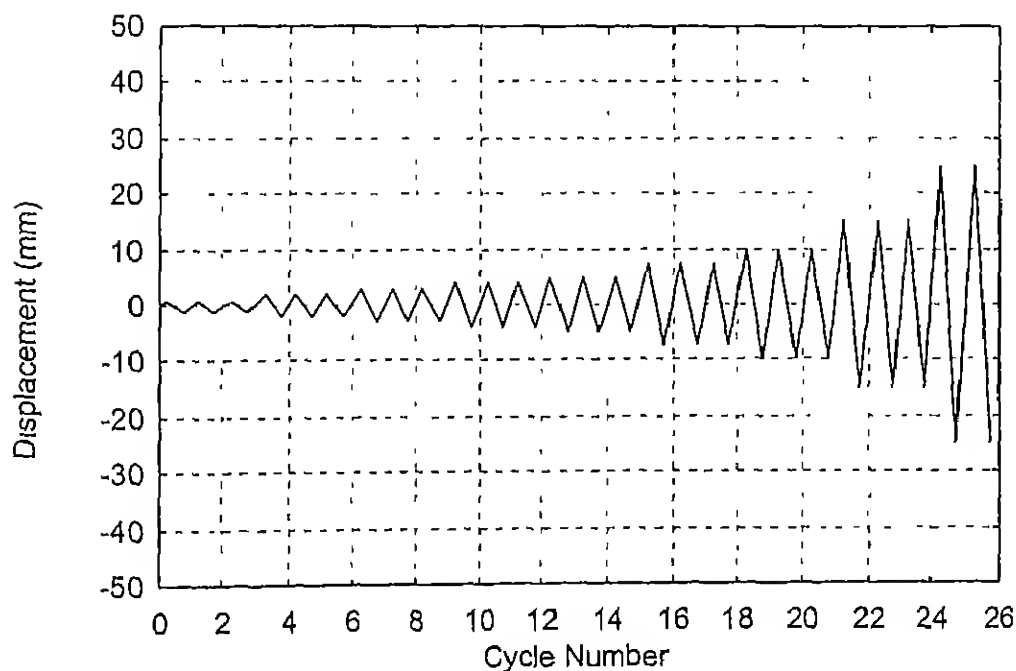


(a) Back Face

Figure 2 8. A schematic of the frame showing the location of strain gauges pasted on the longitudinal reinforcement bars in MRF 2

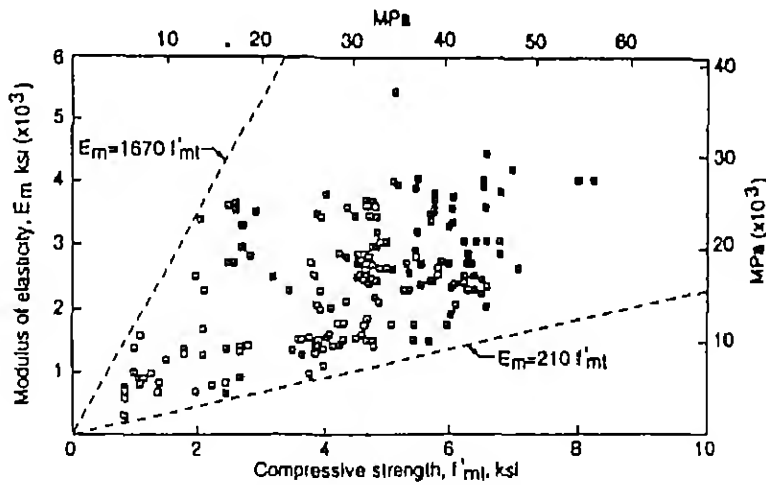


(a) MRF 1 (Infilled Frame)

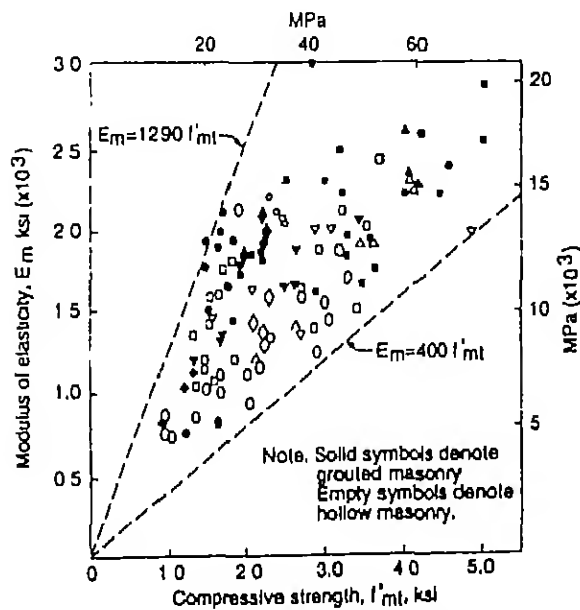


(b) MRF 2 (Bare Frame)

Figure 2.9: Cyclic displacement history applied on (a) MRF 1 and (b) MRF 2.

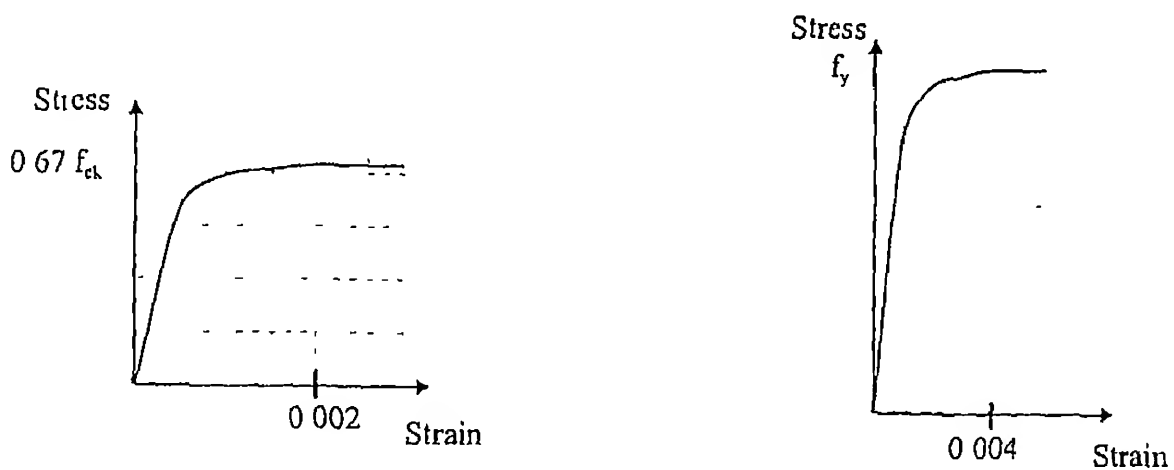


(a) Clay Brick Masonry (Grimm, 1984)



(b) Concrete Masonry (Hamid *et al*, 1987)

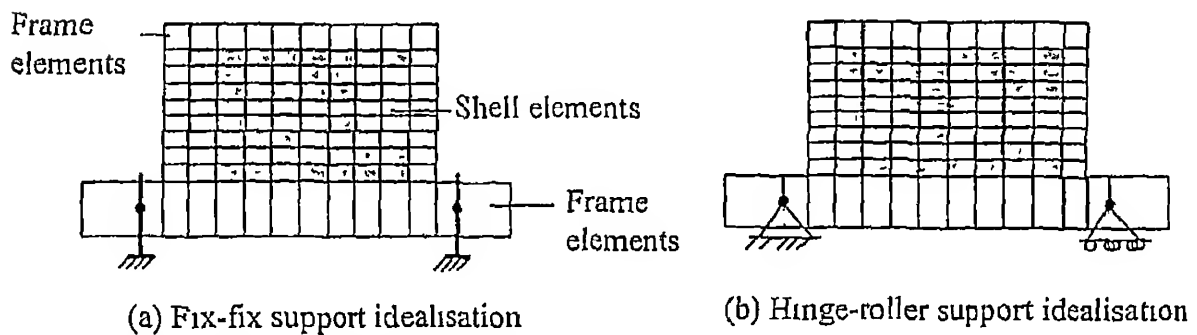
Figure 3.1: Modulus of elasticity of masonry obtained from experiments reported in literature (Drysdales *et al*, 1993). f'_{mt} is prism compressive strength.



(a) Stress-strain curve for concrete

(b) Stress-strain curve for Fe415 steel

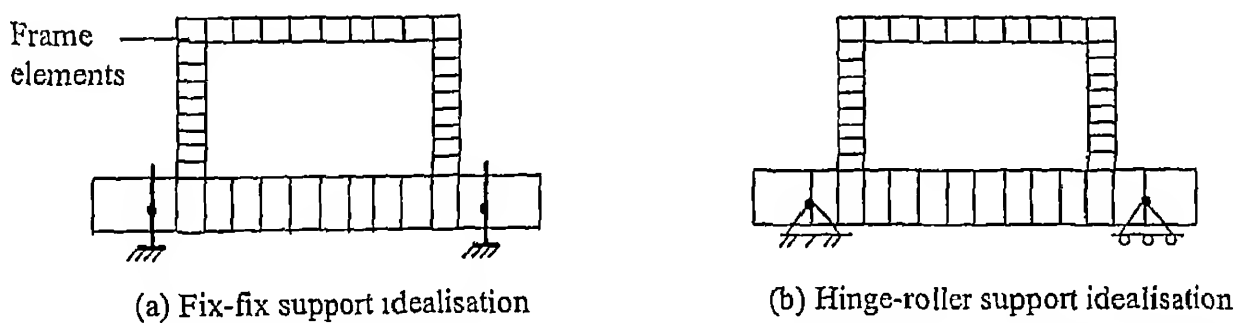
Figure 3.2: Idealized stress-strain curves for concrete and Fe415 steel (IS:456-1978).



(a) Fix-fix support idealisation

(b) Hinge-roller support idealisation

Figure 3.3: Finite element modelling for infill frame for different support conditions using SAP2000



(a) Fix-fix support idealisation

(b) Hinge-roller support idealisation

Figure 3.4: Finite element modelling for bare frame for different support conditions using SAP2000.

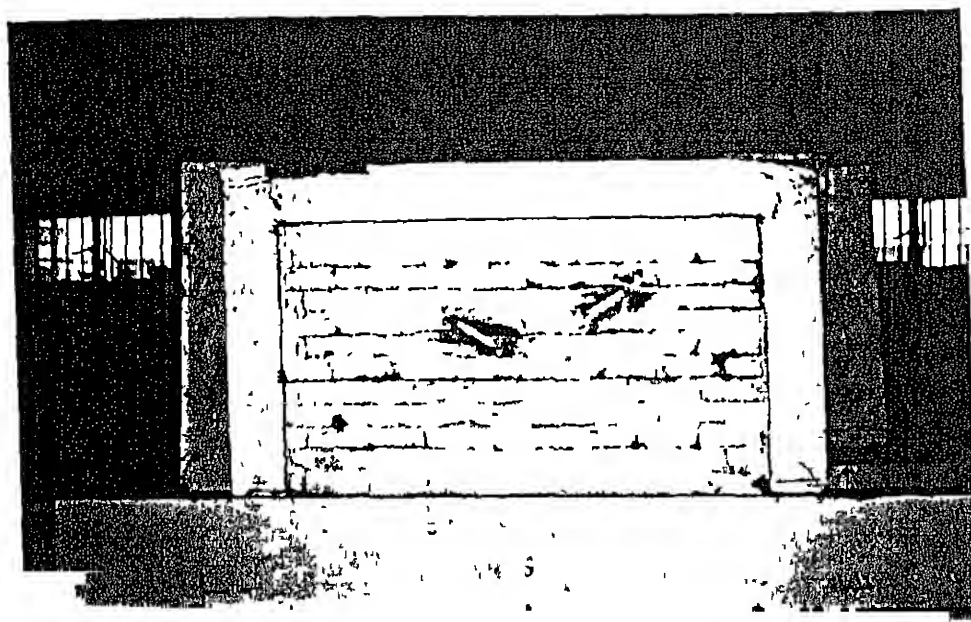


Figure 3.5: Final failure pattern of MRF 1.

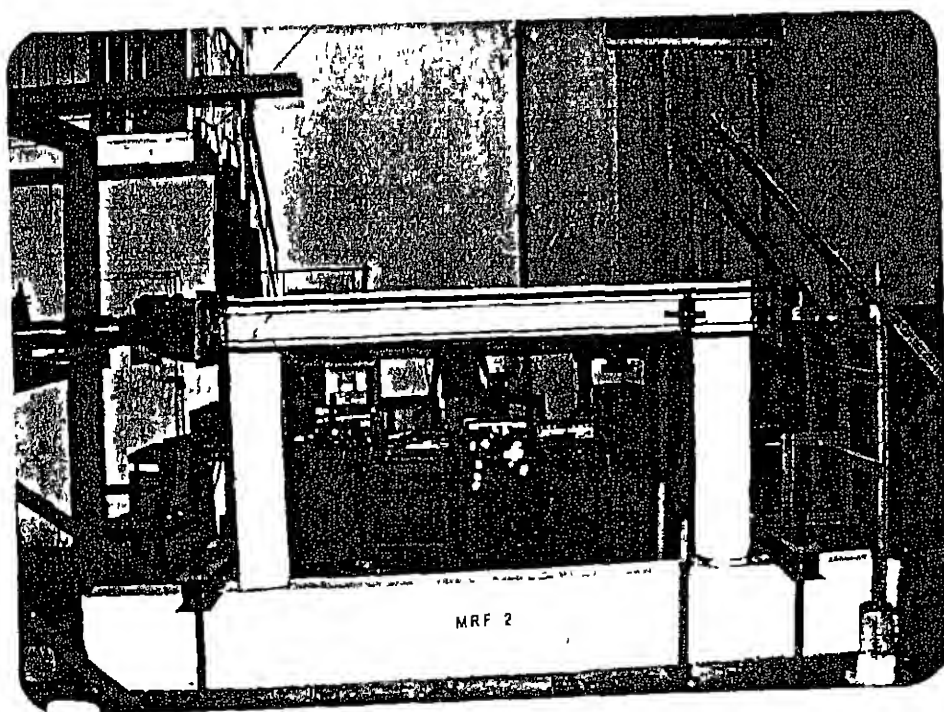
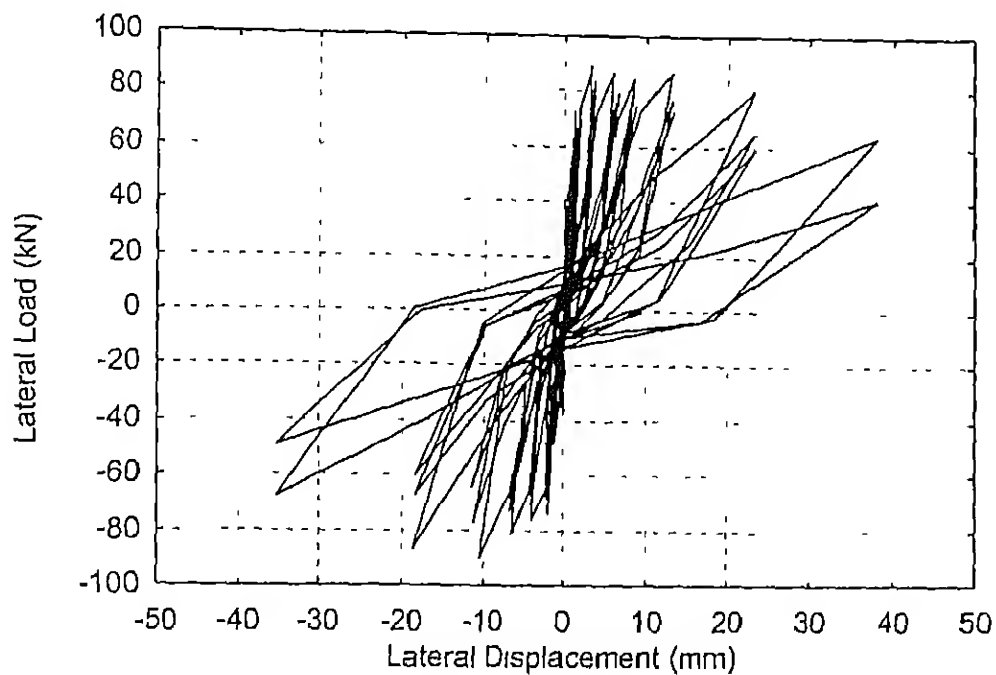
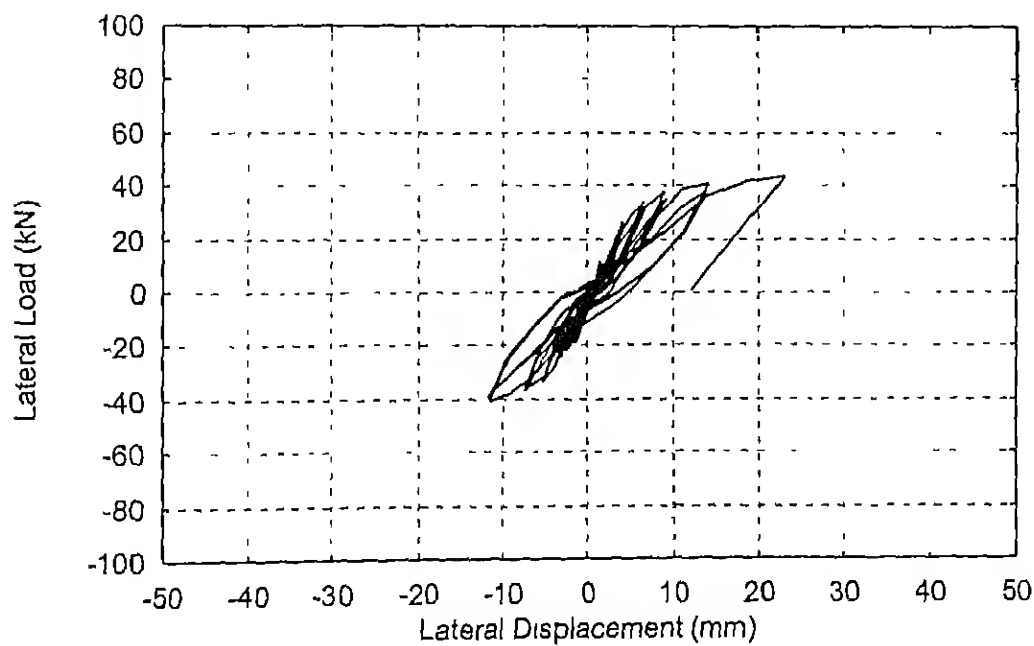


Figure 3.6: Final failure Pattern of MRF 2.



(a) MRF 1 (Infill Frame)



(b) MRF 2 (Bare Frame)

Figure 3.7: Lateral load *versus* lateral displacement hysteresis curves for (a) MRF 1, and (b) MRF 2.

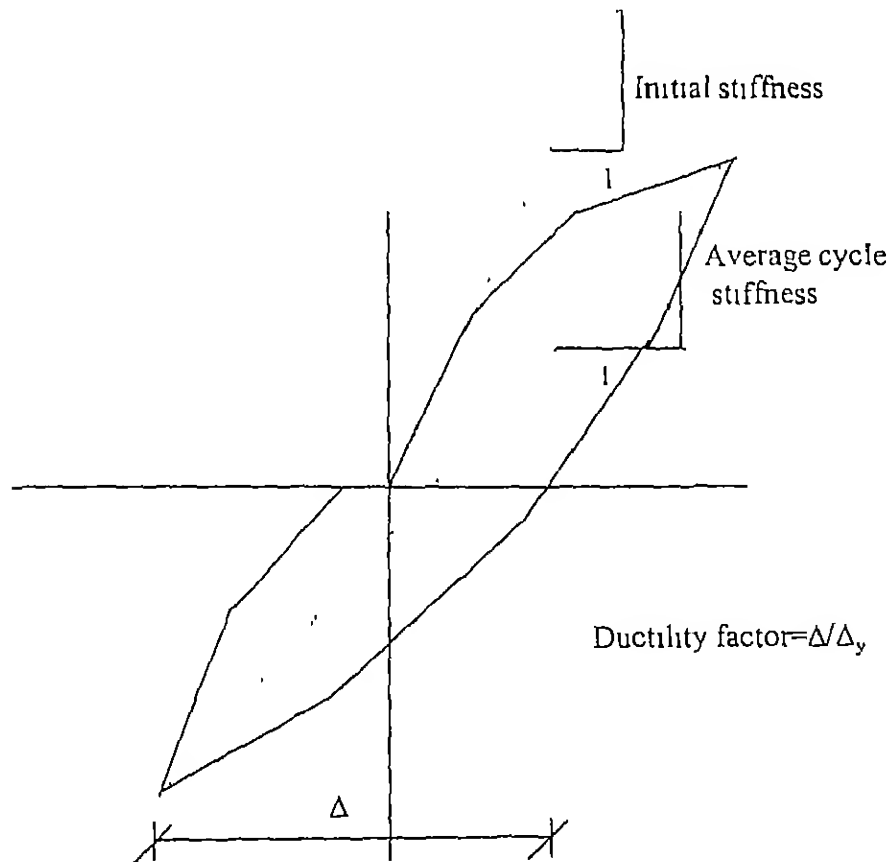


Figure 3.8: Schematic representation of (a) Initial stiffness, (b) Average cycle stiffness and (c) Ductility factor for a cycle.

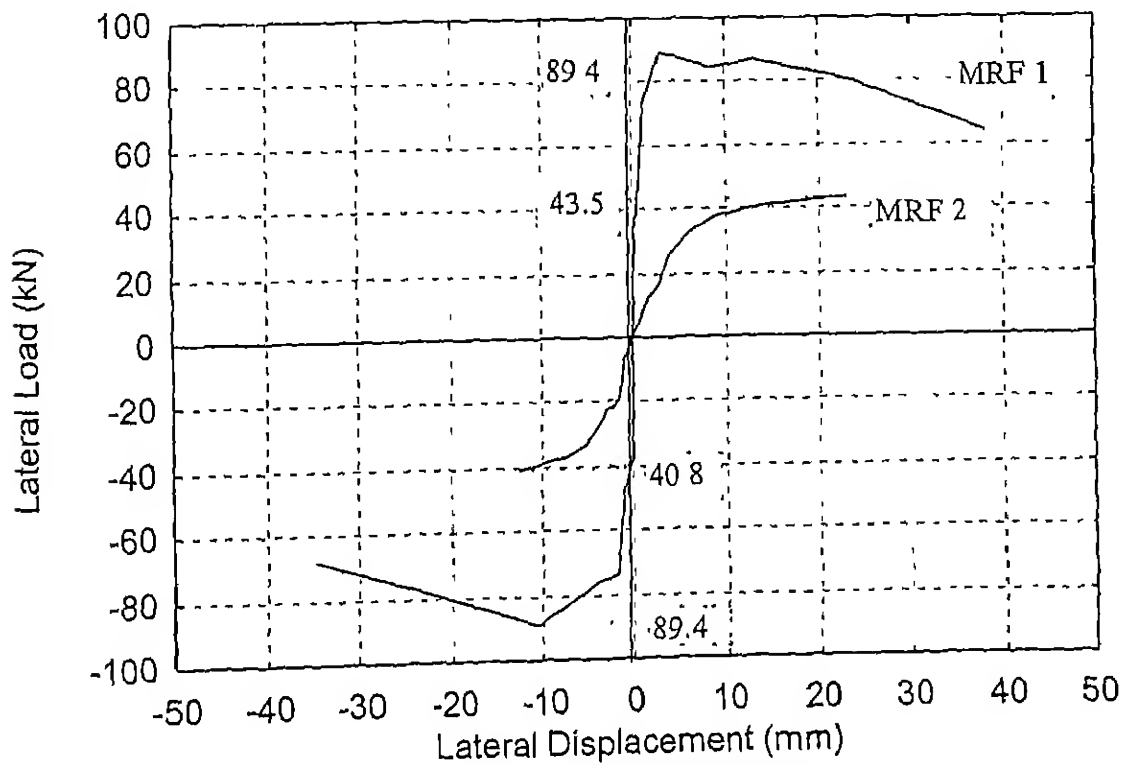
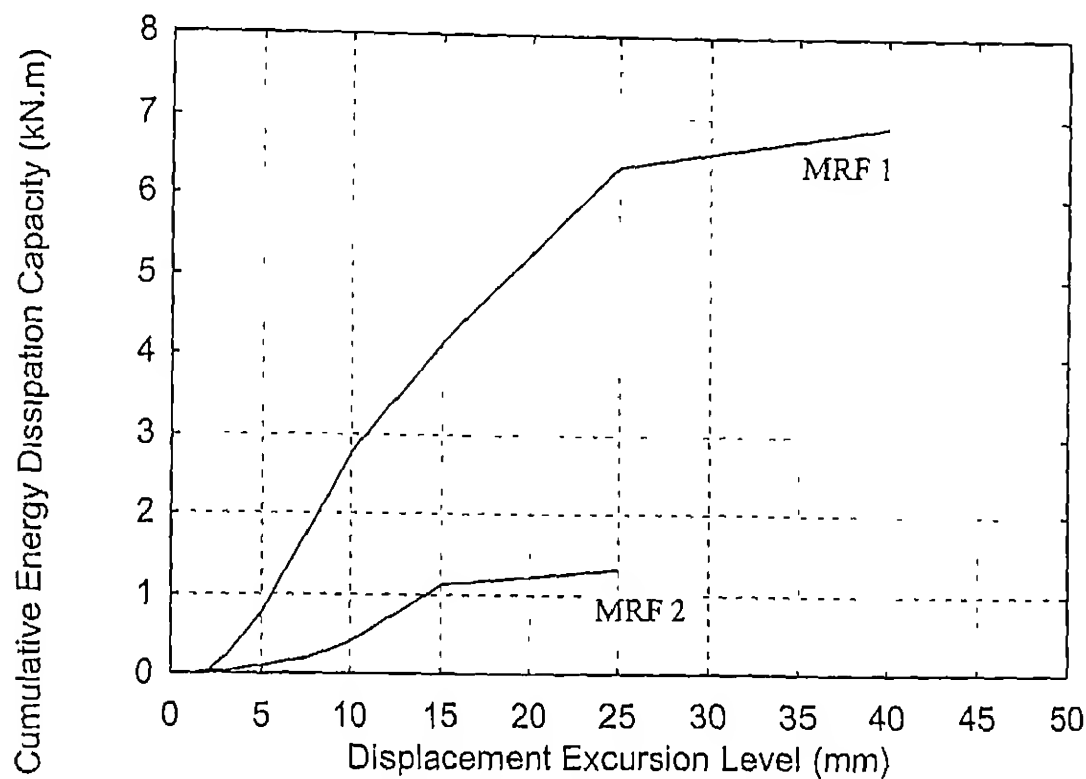
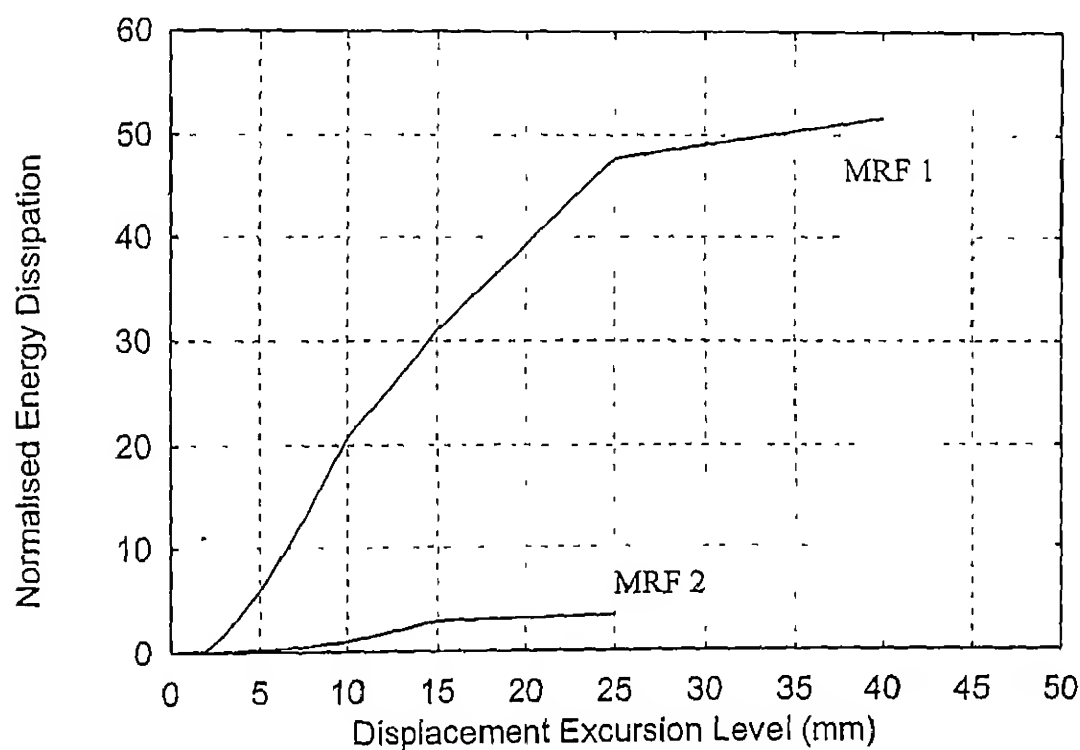


Figure 3.9: Envelope backbone curve of the load displacement hysteresis envelopes of (a) MRF 1 and (b) MRF 2.

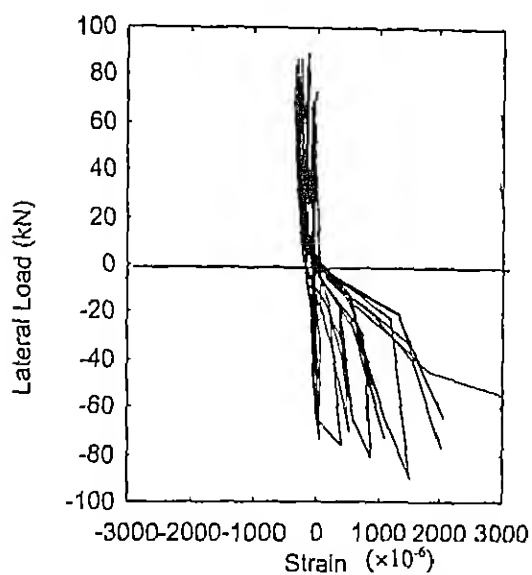


(a) Cumulative Energy Dissipation

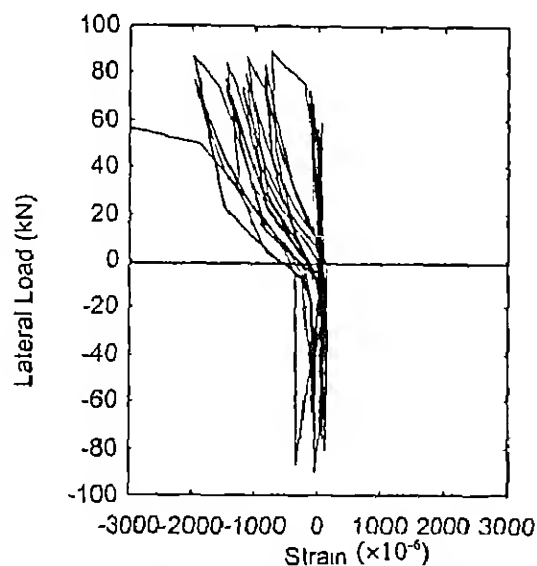


(b) Normalised Energy Dissipation

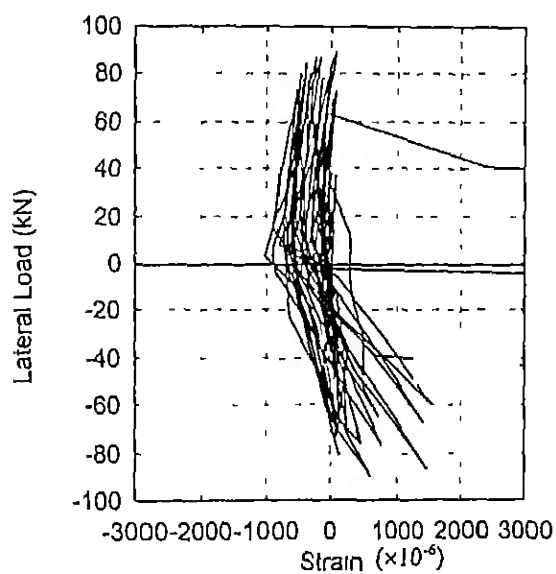
Figure 3.10: Effect of displacement excursion level on energy dissipated in MRF 1 and MRF 2 shown as (a) Cumulative energy dissipated upto that level of displacement excursion, and (b) Cumulative energy dissipated normalised with elastic energy upto yield.



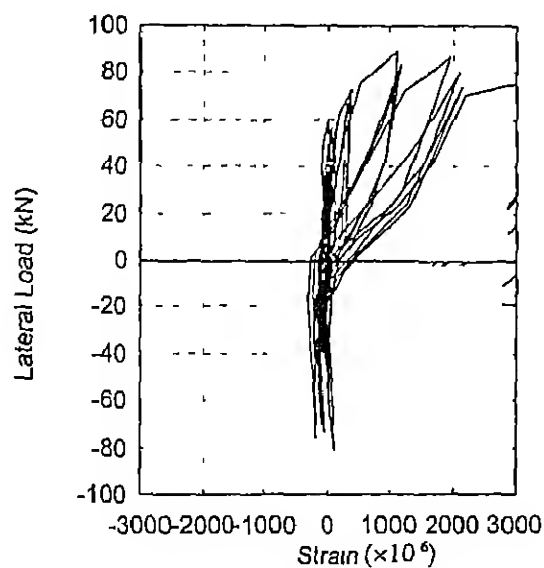
(a) Column Bar at Top (SG17)



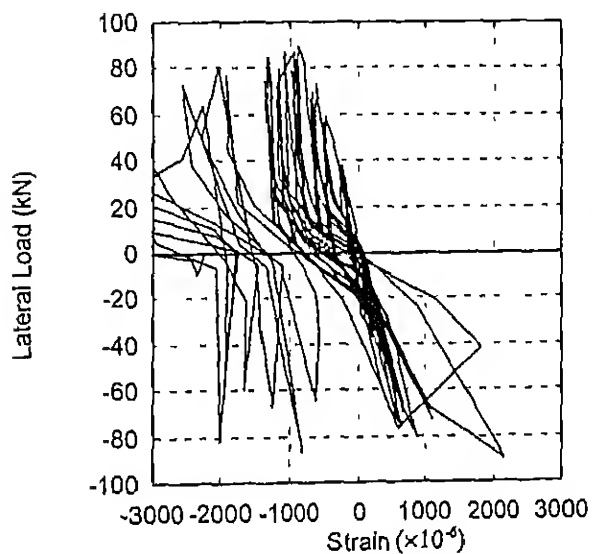
(b) Column Bar at Top (SG14)



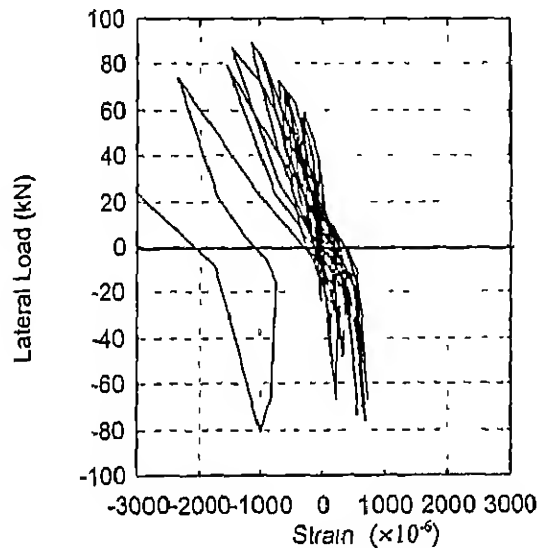
(c) Column Bar at Bottom (SG15)



(d) Column Bar at Bottom (SG3)



(e) Column Bar at Bottom (SG19)



(f) Column Bar at Top (SG2)

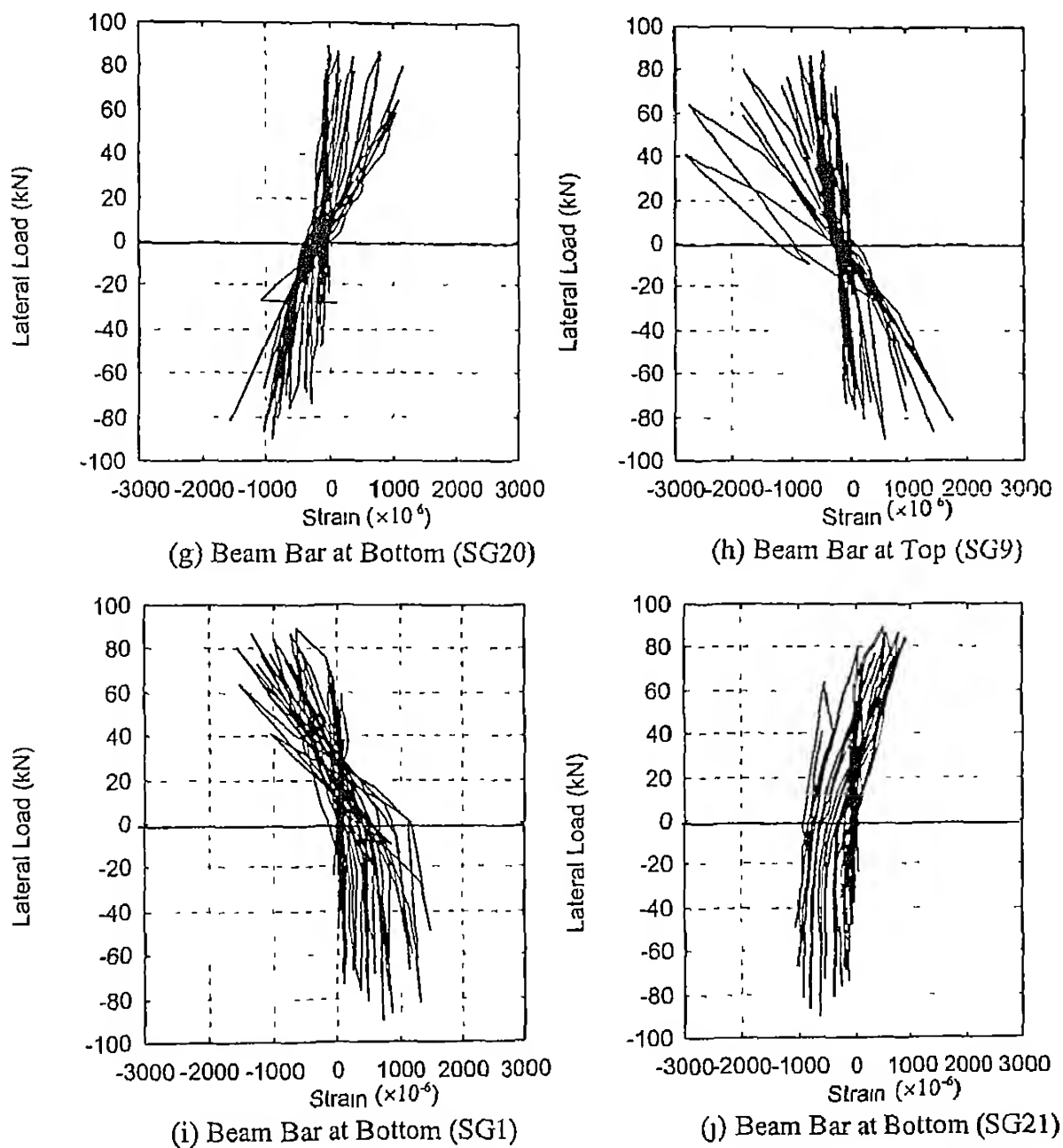
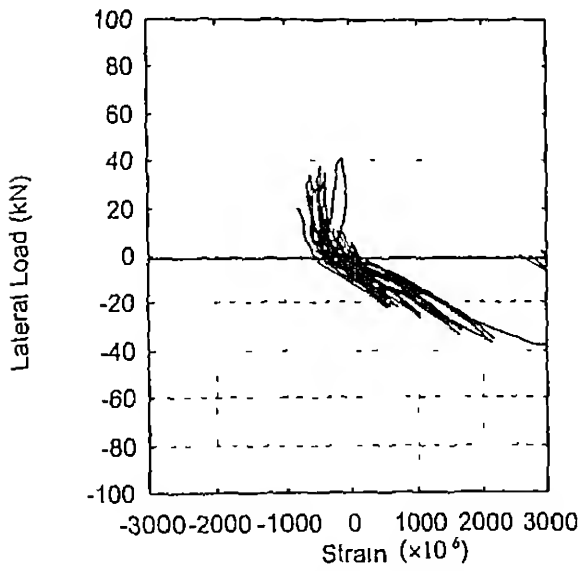
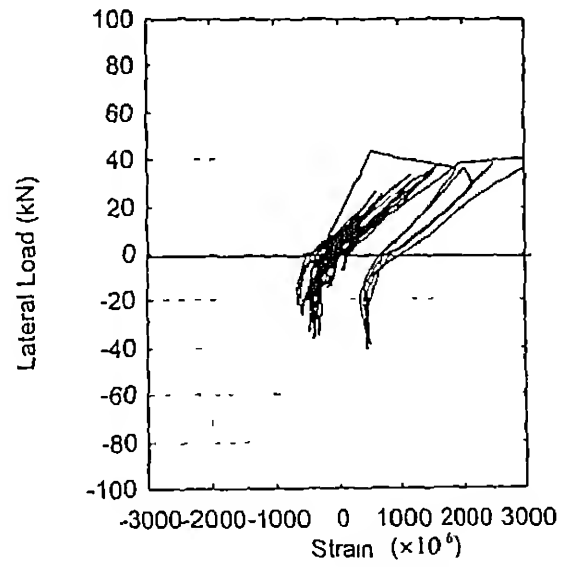


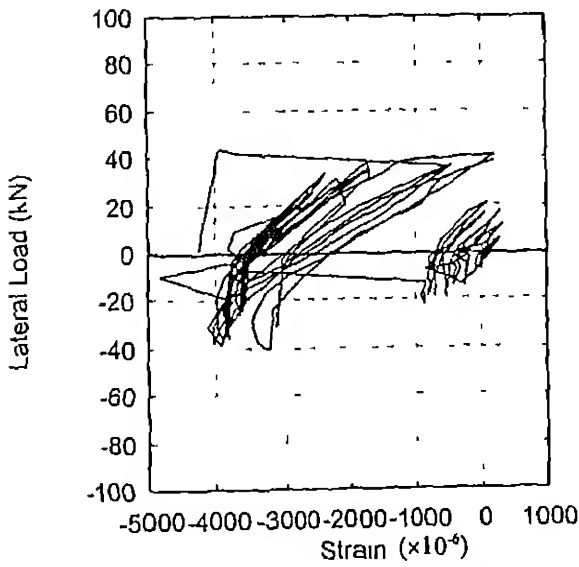
Figure 3.11. Lateral load *versus* bar strain hysteresis curves for reinforcing bars in MRF 1



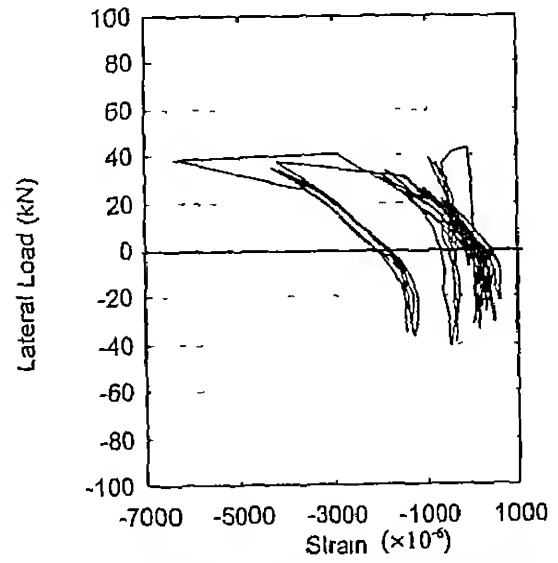
(a) Column Bar at Top (SG17)



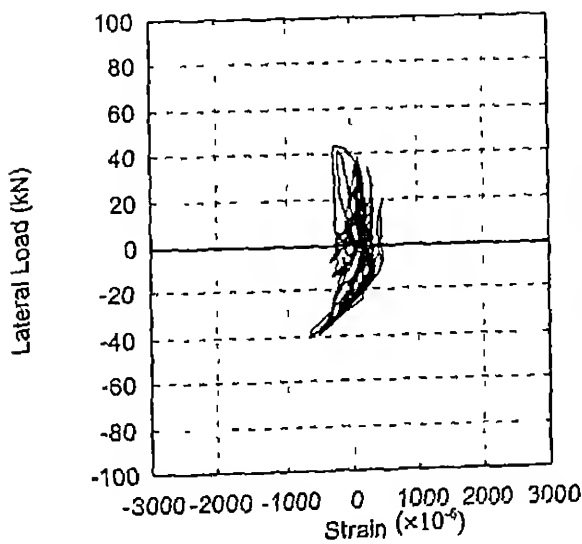
(b) Column Bar at Top (SG19)



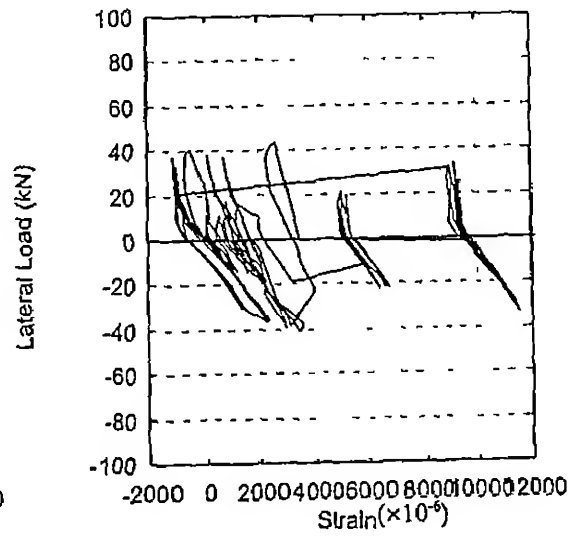
(c) Column Bar at Bottom (SG14)



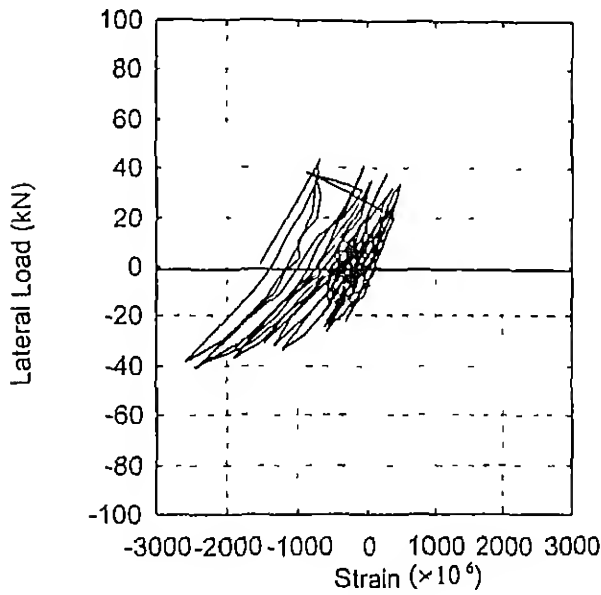
(d) Column Bar at Bottom (SG23)



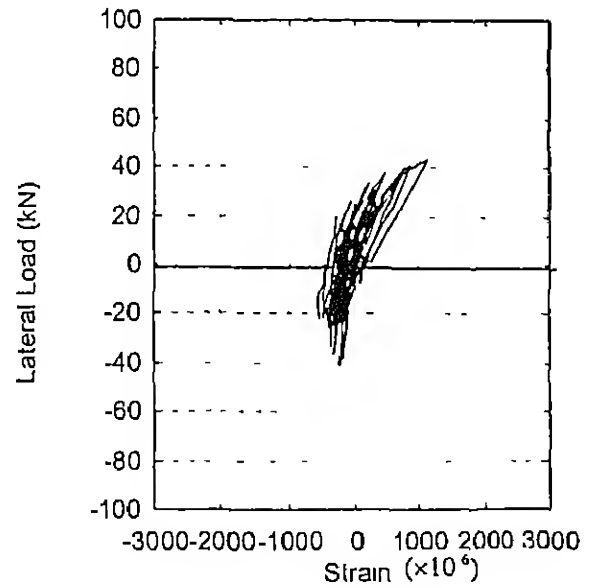
(e) Column Bar at Top (SG4)



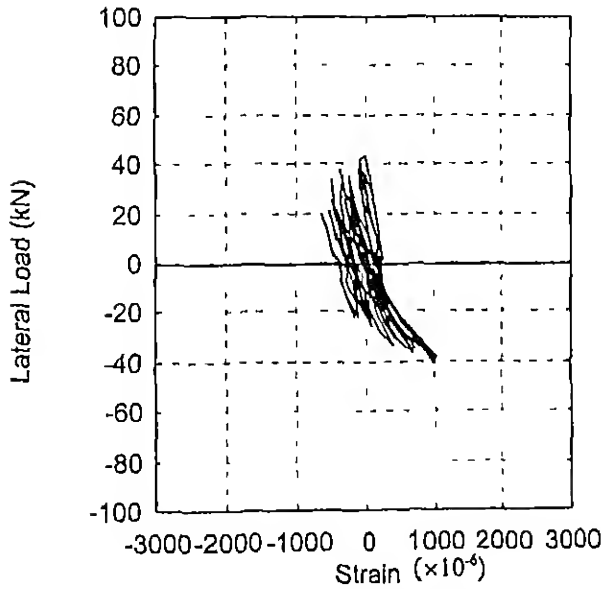
(f) Column Bar at Bottom (SG24)



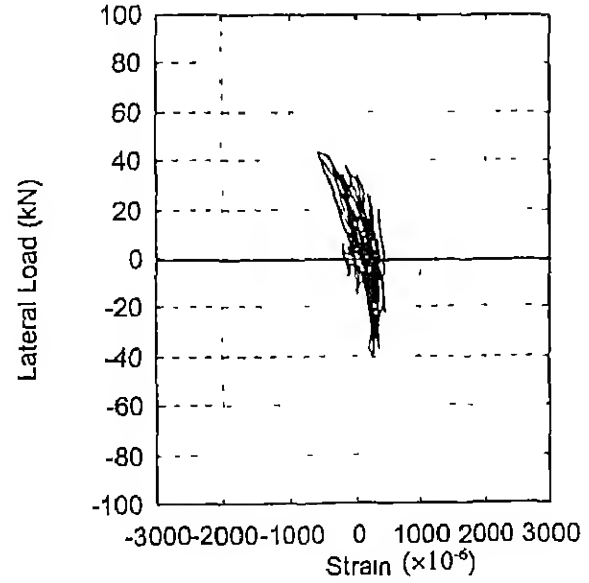
(g) Beam Bar at Bottom (SG12)



(h) Beam Bar at Bottom (SG15)



(i) Beam Bar at Bottom (SG10)



(j) Beam Bar at Top (SG18)

Figure 3.12: Lateral load *versus* strain hysteresis curves for reinforcing bars in MRF 2

Appendix-A

Some observations regarding displacement measured through LVDTs

The following observations have been made by analysing the LVDT data

- (1) The LVDT 2 has been installed for redundancy so that in case, the top edge of the frame gets damaged (where LVDT 1 is fixed), the lateral displacement of the frame can be measured.
- (2) The variation in displacement recorded by LVDT 4 (which has been fixed at the base of the frames) is between -0.79 mm to 0.10 mm for MRF 1 and -0.10 mm to 0.22 mm for MRF 2. From this observation, it is clear that there is negligible sliding of base, as compared to applied displacement cycles
- (3) The LVDT 3 (fixed at the support end of the actuator) has been installed to measure the deflection of the frame on which actuator was installed. The deflection recorded by LVDT 3 varies from -0.72 mm to 0.69 mm for MRF 1, and -0.44 mm to 0.37 mm for MRF 2. These data show that deflection of the actuator frame varies with applied loading, and it is higher for MRF 1 since the load values are higher. On plotting the deflection profile of actuator frame (LVDT 3) with load, comparable stiffness are obtained (Figures A.1 and A.2).
- (4) The load-displacement response has been analysed with respect to load cell output and the net displacement measured from LVDT 1 and LVDT 4 (*i.e.*, the deflection at beam level after taking consideration of slippage at base, if any).
- (5) LVDT 5, installed to measure vertical drift of the base, shows slight variation during the test.

The variation of net displacement with applied displacement excursion levels is shown in Table A for MRF 1 and MRF 2.

Table A. Variation of applied displacements with net displacements for MRF 1 and MRF 2

MRF 1		MRF 2	
Applied Displacement (mm)	Net Displacement (mm)	Applied Displacement (mm)	Net Displacement (mm)
1.00	0.2281	0.99	0.7846
1.02	0.4909	1.02	0.9082
1.05	0.2631	1.05	0.9311
-1.02	-0.094	-0.99	-1.041
-1.02	-0.0468	-0.99	-0.7143
-1.00	-0.1401	-1.00	-0.8371
2.01	1.023	2.02	1.4282
2.01	0.7363	2.02	1.6581
2.01	0.8538	2.10	2.1478
-2.01	-0.065	-2.04	-1.2987
-2.02	-0.300	-2.13	-1.6355
-2.01	-0.220	-2.04	-1.1067
3.00	1.3155	3.00	2.7192
3.00	1.6961	3.00	2.7543
3.00	1.3155	3.00	3.096
-3.00	-1.0653	-3.00	-1.5858
-3.07	-1.1698	-3.00	-1.5162
-3.00	-1.1760	-3.03	-1.6096
5.01	3.0654	4.02	3.4226
5.02	3.5051	4.05	3.7679
5.01	3.5811	3.99	3.4871
-5.02	-2.0165	-4.02	-2.451
-4.99	-2.1561	-4.00	-2.638
-5.04	-2.1004	-3.96	-2.961
7.48	5.8977	4.99	4.189
7.68	6.3606	4.98	4.4874
7.57	5.9861	5.02	4.4228
-7.53	-3.9897	-5.08	-3.411
-7.50	-4.0268	-5.02	-2.9542
-7.54	-4.3076	-5.02	-3.3348
10.02	8.4661	7.47	6.285
10.03	8.2322	7.50	6.4227
10.03	8.7002	7.50	6.9092
-9.99	-6.249	-7.50	-5.3645
-10.05	-6.507	-7.50	-5.05
-10.08	-6.224	-7.53	-4.978
15.18	13.1569	10.05	9.0679
15.30	13.1746	10.08	9.2551
15.38	13.4378	9.99	9.0555
-15.10	-10.4540	-10.02	-7.4817
-15.60	-11.3778	-10.06	-7.096
-15.00	-11.4838	-9.96	-7.3178
25.50	23.3756	15.11	14.1799
25.25	23.4057	14.96	14.0157
25.38	23.5222	14.96	14.0104
-25.18	-18.5195	-15.10	-11.599
-25.39	-18.3210	-15.02	-11.8512
-25.63	-18.3900	-15.09	-11.8512
40.80	38.2684	24.88	23.324
40.47	38.2570	-	-
-42.00	-35.7200	-	-
-40.60	-35.4700	-	-

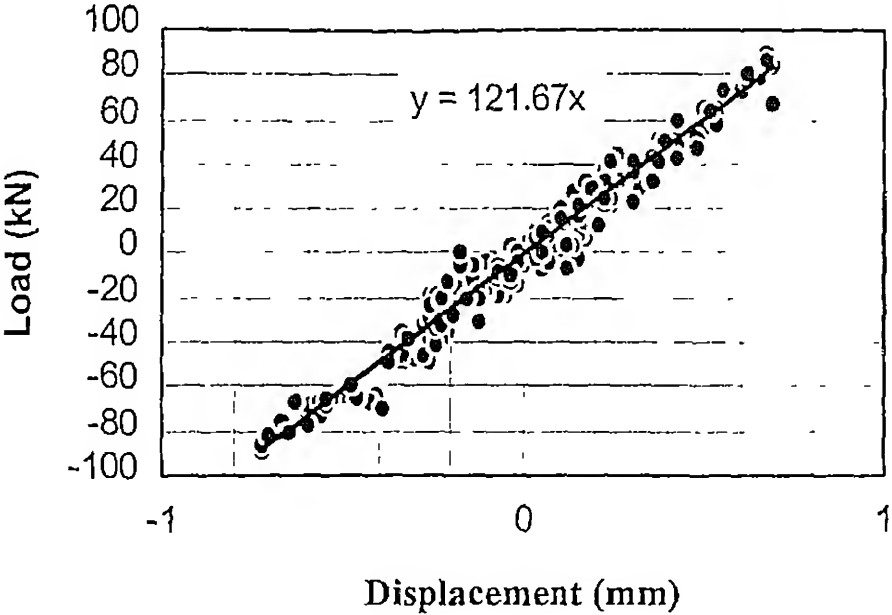


Figure A 1. Plot of LVDT3 data with load for MRF 1

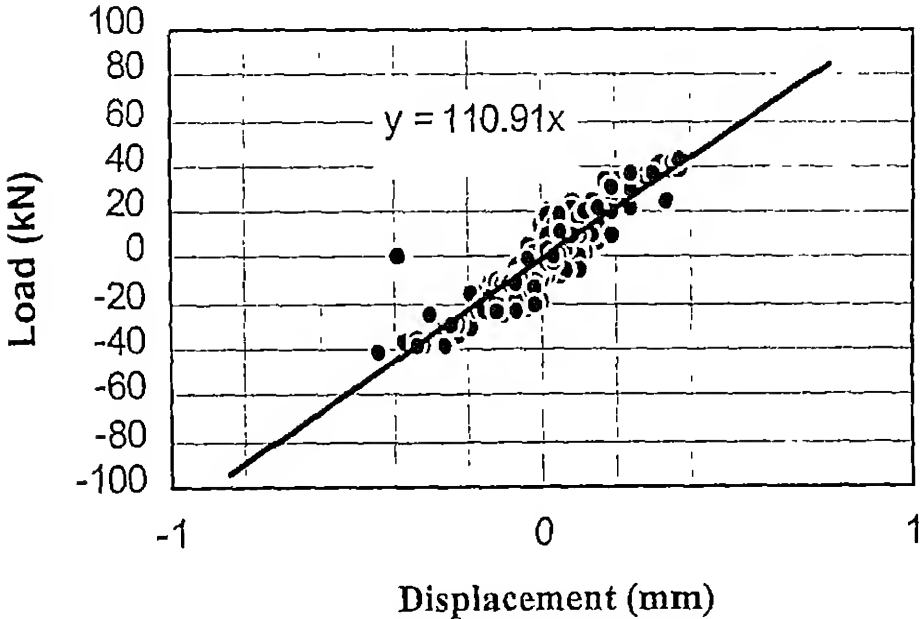


Figure A 2. Plot of LVDT3 data with load for MRF 2

